Plasma metabolomic fingerprint of advanced cirrhosis stages among HIV/HCV-coinfected and HCV-monoinfected patients

Sergio Salgüero , David Rojo, Juan Berenguer, Juan González-García, Amanda Fernández-Rodríguez, Oscar Brochado-Kith, Cristina Díez, Victor Hontañon , Ana Virseda-Berdices, Javier Martínez, Luis Ibañez-Samaniego, Elba Llop-Herrera, Coral Barbas, Salvador Resino, María A Jiménez-Sousa, Escorial Study Group.

Liver Int. 2020 Sep;40(9):2215-2227.

Type of manuscript: Original article

Title: Plasma metabolomic fingerprint of advanced cirrhosis stages among HIV/HCV-coinfected and HCV-monoinfected patients.

Running head: Metabolomic fingerprint in advanced cirrhosis

Authors: Sergio SALGÜERO [1,2]; David ROJO [3]; Juan BERENGUER [4,5]; Juan GONZÁLEZ-GARCÍA [6,7]; Amanda FERNÁNDEZ-RODRÍGUEZ [1]; Oscar BROCHADO-KITH [1]; Cristina DÍEZ [4,5]; Victor HONTAÑON [6,7]; Ana VIRSEDA-BERDICES [1]; Javier MARTÍNEZ [8]; Luis IBAÑEZ-SAMANIEGO [9]; Elba LLOP-HERRERA [10]; Coral BARBAS [3]; Salvador RESINO [1†]; María Angeles JIMÉNEZ-SOUSA [1†*] and the ESCORIAL Study Group.

(†), Authors contributed equally to this work.

Authors' Affiliations:

(1) Unidad de Infección Viral e Inmunidad, Centro Nacional de Microbiología, Instituto de Salud Carlos III, Majadahonda, Madrid, Spain.

(2) Unidad de Análisis Clínicos. Hospital Universitario Fundación Alcorcón. Madrid, Spain.

(3) Centre for Metabolomics and Bioanalysis (CEMBIO), Department of Chemistry and Biochemistry, Facultad de Farmacia, Universidad San Pablo-CEU, CEU Universities, Urbanización Montepríncipe, 28660 Boadilla del Monte. Madrid Spain. .

(4) Unidad de Enfermedades Infecciosas/VIH; Hospital General Universitario "Gregorio Marañón", Madrid, Spain.

(5) Instituto de Investigación Sanitaria Gregorio Marañón (IiSGM), Madrid, Spain.

(6) Servicio de Medicina Interna-Unidad de VIH. Hospital Universitario La Paz. Madrid, Spain.

(7) Instituto de Investigación Sanitaria La Paz (IdiPAZ). Madrid, Spain.

(8) Servicio de Aparato Digestivo, Hospital Universitario Ramón y Cajal, Madrid, Spain.

(9) Servicio de Aparato Digestivo, Hospital General Universitario "Gregorio Marañón", Madrid, Spain.

(10) Departamento de Gastroenterología; Hospital Universitario Puerta de Hierro-Majadahonda; Majadahonda, Madrid; Spain.

***Corresponding author:** Maria Angeles Jiménez-Sousa; Centro Nacional de Microbiología, Instituto de Salud Carlos III (Campus Majadahonda); Carretera Majadahonda-Pozuelo, Km 2.2; 28220 Majadahonda (Madrid); Phone: +34918223862. E-mail: jimenezsousa@isciii.es

Character count of Title: 116

Character count of Running Head: 51

Word count of Abstract: 234

Word count of Keywords: 6

Word count of Text: 4356

Count of References: 58

Count of Tables: 2

Count of Figures: 4

Additional Files: 12

Email addresses:

Sergio SALGÜERO: ssalguerof@hotmail.com

David ROJO: david.rojoblanco@ceu.es

Juan BERENGUER: jbb4@me.com

Juan GONZÁLEZ-GARCÍA: juangonzalezgar@gmail.com

Amanda RODRÍGUEZ-FERNÁNDEZ: amandafr@isciii.es

Oscar BROCHADO-KITH: brochado1993@gmail.com

Cristina DÍEZ: crispu82@gmail.com

Ana VIRSEDA-BERDICES: anavirseda@isciii.es

Victor HONTAÑÓN: victor.hontanon@gmail.com

Javier MARTÍNEZ: martinez.gonzalez.javier@gmail.com

Luis IBAÑEZ-SAMANIEGO: lisamaniego@gmail.com

Elba LLOP-HERRERA: elballop@gmail.com

Coral BARBAS: cbarbas@ceu.es

Salvador RESINO: sresino@isciii.es

María Ángeles JIMÉNEZ-SOUSA: jimenezsousa@isciii.es

List of abbreviations

Human immunodeficiency virus (HIV)

Hepatitis C virus (HCV)

Chronic hepatitis C (CHC)

Child-Turcotte-Pugh score (CTP)

Polymerase chain reaction (PCR)

Combination antiretroviral therapy (cART)

Gas chromatography–mass spectrometry (GC-MS)

Liquid chromatography–mass spectrometry (LC-MS)

Ordinal logistic regression (OLR)

International normalized ratio (INR)

Variable importance in projection (VIP)

Lysophosphatidylcholine (LPC)

Cirrhosis-associated immune dysfunction (CAID)

Direct-acting antivirals (DAAs)

Model for End-stage Liver Disease (MELD)

Quality control (QC)

Principal component analysis (PCA)

Leave-one-out cross-validation (LOOCV)

Partial least squares discriminant analysis (PLS-DA)

Odds ratio (OR)

False discovery rate (FDR)

Intravenous drug user (IVDU)

Relative standard deviation (RSD)

Phosphatidylcholine (PC)

Phosphatidyletanolamine (PE)

Lysophosphatidyletanolamine (LPE)

Branched-chain amino acids (BCAA)

Hepatic stellate cells (HSCs)

Declarations

Competing interests

The authors declare that they have no competing interests.

Funding

This study was supported by grants from Instituto de Salud Carlos III (ISCIII; grant numbers CP17CIII/00007 (MPY407/18) and PI18CIII/00028 (MPY385/18) to MAJS, PI14/01094 and PI17/00657 to JB, PI14/01581 and PI17/00903 to JGG, and PI14CIII/00011 and PI17CIII/00003 to SR) and Ministerio de Sanidad, Servicios Sociales e Igualdad (grant number EC11-241). JB is an investigator from the Programa de Intensificación de la Actividad Investigadora en el Sistema Nacional de Salud (I3SNS), Refs INT16/00100. CB and DR acknowledge funding from the Ministerio de Ciencia, Innovación y Universidades (RTI2018-095166-B-I00).

Acknowledgments

This study would not have been possible without the collaboration of all the patients, medical and nursery staff and data managers who have taken part in the project. We want to particularly acknowledge the support of the HIV BioBank, which is integrated in the Spanish AIDS Research Network and all collaborating Centres for the generous contribution with clinical samples for the present work (see **Appendix**). The HIV BioBank, is supported by Instituto de Salud Carlos III, Spanish Health Ministry (Grant nº RD06/0006/0035, RD12/0017/0037 and RD16/0025/0019) as part of the Plan Nacional R + D + I and cofinanced by ISCIII- Subdirección General de Evaluación y el Fondo Europeo de Desarrollo Regional (FEDER)". The RIS Cohort (CoRIS) is funded by the Instituto de Salud Carlos III through the Red Temática de Investigación Cooperativa en SIDA (RIS C03/173, RD12/0017/0018 and RD16/0002/0006) as part of the Plan Nacional R+D+I and cofinanced by ISCIII-Subdirección General de Evaluacion and the Fondo Europeo de Desarrollo Regional (FEDER).

Abstract

Background & Aims: Hepatitis C virus (HCV), human immunodeficiency virus (HIV), and cirrhosis induce metabolic disorders. Here, we aimed to evaluate the association between plasma metabolites and Child- Turcotte-Pugh (CTP) score in HIV/HCV-coinfected and HCV-monoinfected patients with advanced cirrhosis.

Methods: Observational study in 62 HIV/HCV-coinfected and 28 HCV-monoinfected patients. Metabolomics analysis was performed by gas chromatography-mass spectrometry (GC-MS) and liquid chromatography-mass spectrometry (LC-MS). The statistical association analysis was performed by partial least squares discriminant analysis (PLS-DA) and generalized linear model (GLM) with binomial distribution (to analyze HIV coinfection, high alcohol intake, treatment with statins, previous HCV therapy failure and decompensation) and ordinal logistic regression (OLR) models to analyze different stages of cirrhosis (CTP score).

Results: The statistical analysis identified plasma metabolites associated to HIV coinfection, high alcohol intake, CTP score and hepatic decompensation. Overall, fatty acids, bile acids, aromatic and sulfur amino acids, butyrate derivatives, oxidized phospholipids, energy-related metabolites, and bacterial fermentation-related metabolites were increased in more advanced cirrhosis stages; while lysophosphatidylcholines and lysophosphatidylethanolamines, branched-chain amino acids (BCAA), and metabolites of tricarboxylic acid cycle, among others, were decreased in more advanced cirrhosis. Most of the significant metabolites displayed a similar trend after stratifying for HIV/HCV and HCV infected patients. Glycolic acid, LPC(16:0) and taurocholic acid had high accuracy for discriminating patients according to decompensated cirrhosis (CTP ≥7).

Conclusion: Altered plasma metabolomic profile was associated with advanced stages of cirrhosis in HIV/HCV-coinfected and HCV-monoinfected patients.

Key Words

Chronic hepatitis C; HIV; cirrhosis; Child-Turcotte-Pugh; metabolomics

Background

An estimated 71 million people have hepatitis C virus (HCV) infection worldwide, with a prevalence of 1.5% in the World Health Organization (WHO) European Region [1]. Besides, due to the shared routes of transmission, about 6.2% of people living with human immunodeficiency virus (HIV) have serological evidence of HCV infection [1]. Liver cirrhosis is a common outcome in chronic hepatitis C (CHC) patients and supposes an important risk for liver failure and hepatocellular carcinoma [2], being the progression of the liver disease faster in HIV/HCV-coinfected patients, who have increased rates of liver failure and liver-related mortality [3].

Cirrhosis is an advanced stage of liver disease whose physiopathology is determined by multiple factors, including oxidative stress, systemic inflammation, and organ dysfunction [4,5]. Excessive inflammation can coexist with an immunodeficiency, as part of the cirrhosis-associated immune dysfunction (CAID). The Child-Turcotte-Pugh (CTP) score is a tool widely used for the classification of the cirrhosis severity and to predict the prognosis of patients with chronic liver disease, having a higher sensitivity for liver failure in comparison to other scores [6]. Currently, although there is a reduction in the incidence of HCV-related liver cirrhosis by the effectiveness of new direct-acting antivirals (DAAs), a subgroup of patients remain at risk of progression and developing hepatocellular carcinoma [7]. Additionally, about 40% of patients with HCV infection might be undiagnosed and be identified at a late, decompensated stage, when the therapy of the HCV infection might be less effective to regress the liver disease [8].

Both HCV and HIV infection induce metabolic disorders in cirrhotic patients. The life cycle of HCV is closely associated with lipid metabolism, and this association includes entry into naïve cells, infection, RNA replication, viral assembly, and viral exocytosis [9,10]. Similarly, HIV infection is linked to specific metabolic signatures related to acquired immunodeficiency syndrome (AIDS) progression, microbial translocation, and hepatic function, as well as response to antiretroviral therapy [11,12]. Since cirrhosis may manifest through many different ways, most of the current literature on the identification of key metabolic changes associated to liver cirrhosis contain heterogeneous studies including both viral and non-viral etiology. Besides, to our knowledge, there is no studies about the metabolic profile in different stages of cirrhosis, stratified by CTP score, in HIV/HCV-coinfected and HCV-infected patients. A better understanding of the pathophysiology of the cirrhosis progression produced by HCV may provide a novel insight for the management of these patients.

In this study, we aimed to evaluate the association between plasma specific metabolites and the CTP score in HIV/HCV-coinfected and HCV-monoinfected patients with advanced cirrhosis.

Methods

Study subjects

We performed a cross-sectional study in patients with advanced HCV-related cirrhosis from the cohort ESCORIAL (see **Appendix**) enrolled from January 2015 to June 2016 in Madrid, Spain. This study was performed according to the Declaration of Helsinki and approved by the Research Ethics Committee of the Institute of Health Carlos III (CEI41_2014/CEI42_2020). Before enrollment, participants gave their written informed consent.

The selection criteria were: 1) demonstrable active HCV infection by polymerase chain reaction (PCR); 2) advanced cirrhosis (liver decompensation or liver stiffness ≥25 kPa, or CTP ≥7, or hepatic liver pressure gradient ≥10 mmHg); 3) available CTP score and plasma sample to perform metabolomics analysis. HIV/HCV-coinfected patients had stable combination antiretroviral therapy (cART) ≥6 months and undetectable plasma HIV viral load (<50 copies/mL).

Clinical data

The most relevant epidemiological, clinical, and virological characteristics were collected prospectively using an online form within each center, which fulfilled requirements of data confidentiality. The information stored in the database was monitored for all centers to check that it was in accordance with the patient's medical records.

Our primary outcome was the CTP score, which was calculated from five routine laboratory parameters and clinical measures of liver disease (total bilirubin, serum albumin, international normalized ratio (INR), ascites and hepatic encephalopathy) and hepatic decompensation, which was defined as CTP score ≥7. CTP score can range from 5 to 15 points. As secondary outcomes, we analyzed the differences in the metabolic profile regarding HIV/HCV coinfection (vs. HCV monoinfection), current high alcohol intake (>50 g/day vs. never), treatment with statins (vs. never), decompensated cirrhosis (CTP ≥7 vs CTP <7), and previous anti-HCV therapy (vs. never).

Non-targeted metabolomics

Reagents and standards for metabolomics

The list of reagents and standards is available in **Additional File 1**.

Metabolite extraction and sample preparation

Firstly, samples were inactivated for viruses by mixing methanol with plasma (3:1, v/v). Next, plasma samples were vortexed (15 seg), maintened in cold for 5 min, centrifuged (16000 g, 20 min, 4°C) and freezed at -80°C before the shipment of samples to the Center for Metabolomics and Bioanalysis (San Pablo-CEU University, Pozuelo de Alarcón, Spain). The day of analysis, the samples were processed for their subsequent measurement by gas chromatography-mass spectrometry (GC-MS) and liquid chromatography-mass spectrometry (LC-MS). Quality controls (QCs) samples were prepared independently for each analytical platform by pooling and mixing equal volumes of each corresponding sample (full description in **Additional File 1**).

Data acquisition

Metabolomic analysis was performed by two complementary analytical platforms according to a methodology previously used [13]. A GC system (Agilent Technologies 7890A) was used consisting of an autosampler (Agilent Technologies 7693) and an inert mass selective detector (MSD) with quadrupole (Agilent Technologies 5975). The derivatized samples were injected through a GC-Column DB5-MS (30 m length, 0.25 mm internal diameter, 0.25 μm film 95% dimethylpolysiloxane / 5% diphenylpolysiloxane) with a pre-column (10 m J&W integrated with Agilent 122-5532G). To increase the metabolite coverage, a LC system consisting of a degasser, a binary pump, and an autosampler (1290 infinity II, Agilent) was also used. The samples were injected into a reversed-phase column (Zorbax Extend C18 50 x 2.1 mm, 1.8 μm; Agilent). The mobile phases were solvent A (H_2O containing 0.1% FA) and solvent B (acetonitrile containing 0.1% FA). Data were collected in positive and negative electrospray ionization (ESI) modes in separate runs using Q-TOF (Agilent 6550 iFunnel) (full description in **Additional File 1**).

Data treatment and quality assurance

In GC-MS, the deconvolution and identification were performed using MassHunter Quantitative Unknowns Analysis (B.07.00, Agilent), alignment with MassProfiler Professional software (version 13.0, Agilent), and peak integration using MassHunter Quantitative Analysis (version B.07.00, Agilent). In LC-MS, the Molecular Feature Extraction and the Recursive Feature Extraction algorithms in the MassHunter Profinder software (B.08.00, Agilent) were used for deconvolution and alignment of the raw data. After data reprocessing, the metabolic features were subsequently filtered (quality assurance details are available in **Additional File 1)**.

Markers of bacterial translocation and infection

The following plasma biomarkers were measured by ELISA: i) lipopolysaccharide by a Limulus amebocyte lysate chromogenic endpoint ELISA (LPS; Hycult Biotech, Uden, The Netherlands); ii) lipopolysaccharide-binding protein (LBP) (R&D Systems, Minneapolis, USA); iii) Interleukin 6 (IL6) by ProcartaPlex™ immunoassay (Bender MedSystems GmbH, Vienna, Austria) according to the manufacturer's specifications using a Luminex 200™ analyzer (Luminex Corporation, Austin, TX, United States).

Statistical analysis

The statistical analysis was carried out with MetaboAnalyst 4.0 software (http://www.metaboanalyst.ca/), Statistical Package for the Social Sciences (SPSS) 22.0 software (IBM Corp., Chicago, USA), and R statistical package version v3.4.3 (R Foundation for Statistical Computing, Vienna, Austria).

For the descriptive study, categorical data were analyzed using the chi-square test, and continuous variables using the Kruskal-Wallis test. For the metabolomic analysis, before performing the differential analysis, variables were log-transformed (log_2) and auto-scaled. Study reliability was analyzed by plotting patients and quality controls together via unsupervised principal component analysis (PCA). Next, we performed a supervised multivariate analysis by partial least squares discriminant analysis (PLS-DA), which models all biomarkers together. The optimal number of components for the model was determined by cross-validation with leave-one-out cross-validation (LOOCV) method using R^2 and Q^2 values as performance measures. The PLS-DA model provides the variable importance in projection (VIP) score for each metabolite. Permutation was carried out by separation distance (B/W) with a permutation number of 1000 to confirm the validity of the model.

For analysis of association, we used generalized linear model (GLM) with binomial distribution (logit-link) and ordinal logistic regression (OLR) models to analyze the association of metabolites with dichotomous (HIV coinfection, high alcohol intake, treatment with statins, decompensation, previous HCV therapy failure) ('glm function' in R) and ordinal (CTP score) ('ordinal package' in R) outcome variables, respectively. This test provides the odds ratio (OR) and its level of significance. P-values were corrected for multiple testing by using the false discovery rate (*FDR*) with Benjamini and Hochberg procedure ('qvalue package' in R). Those metabolites with q-value<0.1 in the univariate model were analyzed by multivariate models adjusted by the main clinical and epidemiological baseline characteristics (age, gender, tobacco, alcohol, intravenous drug user (IVDU), previous anti-HCV therapy,

treatment with statins, HCV genotype 3, HCV-RNA > 850,000 IU/mL, CTP score and HIV coinfection), which were previously selected by a stepwise method (forward). When some of these covariates were included in the model as outcome, they were omitted as covariates. P-values were also corrected for multiple testing by using the *FDR* procedure.

Metabolites associated significantly with CTP score in the adjusted model were analyzed also for hepatic decompensation (CTP <7 vs. CTP ≥7) by GLM with binomial distribution. Next, we analyzed the diagnostic performance of significant metabolites resulting from adjusted GLM model by stepwise algorithm for predicting decompensation using the area under the receiver-operating characteristic (AUROC) curve. The following criteria for levels of accuracy were taken into account: >0.90–1 = excellent, >0.80–0.90 = good, >0.70–0.80 = fair, and >0.60–0.70 = poor. Delong test was carried out to compare the AUROC curves.
Finally, we used the list of metabolites resulting from the PLS-DA (VIP ≥1) and adjusted OLR (q-value <0.05) to make a heatmap of metabolites significantly related to CTP score (distance measure: euclidean; clustering algorithm: ward).
Spearman correlation was carried out to investigate the relationship between bacteria-related metabolites and markers of bacterial translocation and infection.

Metabolite identification

The significant metabolites were identified based on FiehnLib [14], NIST 14 libraries, and CEU Mass Mediator search tool (http://ceumass.eps.uspceu.es) [15]. The metabolites are reported in agreement with the criteria of the Metabolomics Standards Initiative [16,17]. Further details are available in **Additional File 1**.

Results

Patient characteristics

Clinical and epidemiological characteristics of 90 patients with advanced HCV-related cirrhosis (62 HIV/HCV-coinfected and 28 HCV-monoinfected patients) are shown in **Table 1**. Overall, the median age was 52.9 years, 70% were male, 8.9% reported a current high intake of alcohol, 58.9% were IVDU, and 48.9% had previously failed antiviral therapy (25% IFN+RBV; 79.5% pegIFN+RBV; 22.7% telaprevir and 6.8% boceprovir; note that some patients received several previous HCV treatments). When patients were stratified by CTP score, patients in more advanced stages had higher values of Model for End-stage Liver Disease (MELD), liver stiffness, hepatic liver pressure gradient, decompensation, as well as higher percentage of HCV genotype 3 and HCV-RNA viral load >850,000 IU/mL.

Reliability analysis

PCA showed that quality control (QC) samples were tightly clustered together in the middle of the plot, confirming the signal stability and technical reproducibility (see **Additional File 2**). The percentage of absences in QC samples was lower than 10% for all platforms.

Association analysis

A) HIV/HCV coinfected patients vs. HCV monoinfected patients

A supervised multivariate analysis by PLS-DA was performed for features detected in GC-MS (R^2=0.619 and Q^2=0.336; four components), LC-MS ESI+ (R^2=0.536 and Q^2=0.102; three components) and LC-MS ESI- (R^2=0.107 and Q^2=-0.015; one component). However, PLS-DA was validated by permutation only for GC-MS (p=0.002) (**see Additional File 3**). Besides, lower levels of cholesterol (OR=0.06; q=0.023), stearic acid (OR=0.08; p=0.023), lysophosphatidylcholine (LPC)(18:0) (OR=2.78; p=0.023), phosphatidylcholine (PC)(16:0/9:0(CHO)) (OR=0.15; p=0.023), and acetylcarnitine (OR=0.22; p=0.023) were significantly associated with HIV coinfection in GLM models (**Additional File 4**).

B) Current high alcohol intake

We investigated the role of high alcohol intake (>50 g/day) on the metabolic fingerprint of patients with advanced HCV-related cirrhosis by comparing patients with current high alcohol intake vs. patients who never had high consumption. The multivariate analysis by PLS-DA was only validated by permutation for GC-MS (R^2=0.777 and Q^2=0.539 with three components and p=0.030 in the validation) (**Additional File 5**). 2,3-butanediol, 2-hydroxy-3-methylbutyric acid, and threonic acid showed a trend to significance in the unadjusted regression model

[OR=6.68 (q=0.058), OR=16.63 (q=0.085), and OR=0.17 (q=0.058), respectively]. 2-hydroxy-3-methylbutyric acid showed significantly higher levels in those patients with high alcohol intake in the adjusted regression model, when FDR was applied (OR=15.50, p=0.028) (**Additional File 6**).

C) Treatment with statins

Ten percent of patients were treated with statins. We found no differences in plasma metabolites when comparing statin-treated vs. untreated patients by PLS-DA and an GLM with binomial distribution (data not shown).

D) Previous HCV therapy failure

When we carried out a multivariate analysis by PLS-DA, we found no differences in plasma metabolites between patients who failed previously to HCV therapy and who did not fail (data not shown). When we carried out GLM models, two features had q<0,1, however, none of them could be identified (**Additional File 7**).

E) CTP score

A supervised multivariate analysis by PLS-DA was performed for features detected in GC-MS (R^2=0.670 and Q^2=0.117; five components), LC-MS ESI+ (R^2=0.533 and Q^2=0.025; three components) and LC-MS ESI- (R^2=0.560 and Q^2=0.101; three components). PLS-DA was validated by permutation for GC-MS (p=0.045) and LC-MS ESI+ (p=0.025) (see **Additional File 8**). Next, 20 and 11 metabolites with VIP ≥1 could be identified for GC-MS and LC-MS ESI+, respectively (**Figure 1; Additional File 9**).

OLR analyses were performed for each of the metabolites detected and 51 significant features were found, of which 16 had q-value <0.1 after controlling by multiple testing. Of them, 15 features remained significant when adjusted OLR analyses were carried out and only eight metabolites could be identified (**Additional File 10**). Briefly, glycolic acid and taurocholic acid were significantly associated with an elevated CTP score [aOR=2.66 (q=0.001) and aOR=3.62 (q=0.001)], respectively). On the contrary, LPC (20:3), LPC(18:0), LPC(16:0), LPC(20:4), LPC(22:6) and LPE (22:6) were significantly associated with a decreased CTP score [aOR=0.36 (q=0.002); aOR=0.42 (q=0.002); aOR=0.32 (q=0.001); aOR=0.39 (q=0.003); aOR=0.32 (q=0.001); and aOR=0.46 (q=0.006) respectively] (**Table 2**). When patients were stratified by HIV coinfection (**Figure 2**), all metabolites except glycolic acid remained significant for HIV/HCV-coinfected patients, and glycolic acid and taurocholic acid remained significant for HCV-monoinfected patients, and LPC(20:3), LPC(20:4), LPC(22:6) and LPE(22:6) tended to the significance (**Figure 2**).

Besides, we also evaluated significant metabolites resulting from OLR model according to decompensated cirrhosis (CTP ≥7) (**Additional File 11**). Higher levels of glycolic acid and taurocholic acid (aOR= 6.28, q=0.020 and aOR=4.52, q=0.023, respectively) and lower levels of LPC(20:3), LPC(16:0), and LPC(20:4) (aOR=0.06,q=0.032; aOR=0.11, q=0.020; aOR=0.03, q=0.032, respectively) were associated with decompensated cirrhosis. Next, we selected by adjusted GLM model with stepwise algorithm, glycolic acid, LPC(16:0), and taurocholic acid, as the most significant metabolites. The AUROC of these three metabolites individually was 0.730, 0.689 and 0.769, respectively. However, the AUROC of the three metabolites combined together was 0.879, which was significantly higher that the value obtained for glycolic acid and LPC(16:0) separately (p=0.012 and p=0.009, respectively) (**Figure 3**).

In summary, fatty acids, bile acids, aromatic and sulfur amino acids, butyrate derivatives, oxidized phospholipids, energy-related metabolites, and bacterial fermentation-related metabolites were increased in more advanced cirrhosis stages. In contrast, LPCs and lysophosphatidylethanolamines (LPEs), branched-chain amino acids (BCAA), and metabolites of tricarboxylic acid cycle, among others were decreased in more advanced cirrhosis (**Figure 4**).

F) Correlation between bacteria-related metabolites and markers of bacterial translocation and infection

N-(2-hydroxyethyl) iminodiacetic acid was correlated with LPS (p=0.016) and 3-hydroxybutyric acid with LBP (p=0.012). 2-Hydroxy-3-methylbutyric acid and 2,3-Butanediol were correlated with IL6 (p=0.008 and p<0.001, respectively) (**Additional File 12**).

Discussion

To date, there is scarce information about how the metabolomic profile changes during different stages of HCV-related cirrhosis. In this study, we evaluated the plasma metabolomic profile of patients with advanced HCV-related cirrhosis, finding multiple metabolites that could be involved in biological processes related to liver disease progression. Similar trend, with different strength, was observed for most of the significant metabolites in HIV/HCV-coinfected patients and HCV-monoinfected patients. Glycolic acid, LPC(16:0) and taurocholic acid had high accuracy for discriminating patients according to decompensated cirrhosis (CTP ≥7). To our knowledge, this is the first study investigating the plasma metabolome among cirrhotic HIV/HCV-coinfected patients.

When we compared HIV/HCV coinfected patients versus HCV monoinfected patients, we found that HIV/HCV coinfected had lower cholesterol, stearic acid, PC(16:0/9:0(CHO)) and acetylcarnitine and higher LPC(18:0) levels than HCV monoinfected patients. Both HIV and HCV can alter lipid metabolism. Specifically, hypocholesterolemia has been described both in HIV/HCV coinfected and in HCV monoinfected patients, however lower level has been found in HIV/HCV coinfected compared to HCV monoinfected patients [18], as observed in our study. Besides, previous studies have described lower plasma carnitine levels in HIV-infected patients [19] and higher level of the saturated stearic acid isomer LPC(18:0) in cART/HIV-exposed infants [20]. All of the above supports the results found in this study. Additionally, note that HIV patients included in this study were patients with long-term suppressive ART and an important immune recovery.

By multivariate analysis, three metabolites were linked to high alcohol intake with an elevated VIP score among patients with advanced HCV-related cirrhosis. It was corroborated by adjusted regression models, with which a significantly higher level of 2-Hydroxy-3-methylbutyric acid was found in those patients with high alcohol intake. To our knowledge, this is the first study that identify the association of 2-Hydroxy-3-methylbutyric acid with alcohol intake. This metabolite has been correlated with procalcitonin [21], which identifies cell injury in acute liver failure [22].

LPCs are decisive signaling molecules implicated in controlling cellular proliferation and inflammation [23]. In our study, LPC(16:0), LPC(16:1), LPC(18:0), LPC(20:3), LPC(20:4), LPC(22:6) were downregulated in patients with higher CTP scores. These findings are in agreement with previous studies, in which a lipidomic profile with generalized decrease in circulating LPC species has been described in other inflammatory/immune diseases, such as

obesity [24], type 2 diabetes [25], chronic ischemic stroke [23] and Alzheimer's disease [23]. Moreover, increased lysophospholipase levels have been observed in advanced cirrhosis and hepatocellular carcinoma in previous studies [26,27], so the decreased LPCs level observed in our study could illustrate a higher consumption of LPCs by lysophospholipase enzyme as the molecular mechanism for lower LPCs in advanced HCV-related cirrhosis. Also, we found a similar profile for LPE(22:6), which is an additional metabolite associated with abnormal phospholipid metabolism.

Oxidative stress, defined as the imbalance between oxidant and antioxidant agents, has been involved in the progression of liver disease [28]. Similarly, both HCV replication and HIV infection contribute to oxidative stress [29,30]. In our study, several significant metabolites are involved in the misbalance between the production of free radicals and antioxidant defenses. Both threonic acid and glycolic acid are derived from dehydroascorbic acid by oxidation [31,32]. Oxidized phospholipids, such as PC(16:0/9:0(CHO)), are generated under conditions of oxidative stress. Tyrosine isomers are biological markers of oxidative stress and their accumulation can alter cellular homeostasis and promote disease pathogenesis [33]. Additionally, other significant metabolites involved in oxidative stress, such as 5-oxoproline and aminomalonic acid, are also implicated in the cirrhosis progression [34,35]. Thus, redox imbalance seems a key mechanism in the progression of HCV-related cirrhosis among HIV/HCV and HCV infected patients.

Higher free fatty acids (palmitic acid, oleic acid, stearic acid, palmitoleic acid, and lauric acid) and glycerol levels were detected in patients with the highest CTP scores. In this setting, HCV-infected cells seems to have an impaired peroxisomal function, leading to an accumulation of fatty acid and facilitating HCV viral replication [36]. Regarding liver disease, it has been described that chronic hepatic disease itself alters fatty acid metabolism promoted by gut microbiota [37], among others. Additionally, increased glycerol levels have been previously found in advanced chronic liver disease and hepatocellular carcinoma [38]. Thus, according to our results, cirrhotic HIV/HCV and HCV infected patients showed a similar profile to that described for advanced cirrhosis of different etiologies.

Although the role of butyrate derivatives has not been previously described in the HCV-related cirrhosis, they seem to have an important role in the cirrhosis progression, since several derivatives were found elevated in patients with higher CTP scores. The 2-hydroxybutyrate is a biomarker for insulin resistance [39], whose increase might suggest a more dysregulated glucose metabolism in more advanced HCV-related cirrhosis, according to our results. 3-hydroxybutyrate is a ketone body synthesized in the liver from fatty acids [40], which

has been used as marker of multi-organ failure in patients with alcoholic hepatitis [41], but it has not been previously described in HCV-related cirrhosis. Additionally, 2,3-butanediol, a bacterial fermentation product mainly found in *Enterobacter, Klebsiella, Bacillus* and *Serratia* genera [42], was increased in patients with more advanced cirrhosis. This metabolite may reflect changes in microbiota diversity and disease susceptibility. In fact, increased abundance of *Klebsiella* in blood has been found in patients with hepatocellular carcinoma [43]. Besides, N-(2-hydroxyethyl)-iminodiacetic acid, other significant metabolite in our study, has been correlated with a specific microbiota community [44]. In this study, N-(2-hydroxyethyl) iminodiacetic acid and 3-hydroxybutyric acid were correlated with LPS and LBP, respectively, which are markers of bacterial translocation. This process is a significant complication in HCV-infected patients with cirrhosis, where intestinal permeability, gut-associated lymphatic tissue, and bacterial overgrowth is altered and damaged. Besides, 2-Hydroxy-3-methylbutyric acid and 2,3-butanediol were correlated with IL6, which has been described as a marker with a high diagnostic value for the differentiation of bacterial infection in patients with cirrhosis [45].

Regarding amino acids, we found an elevated level of methionine and tyrosine in patients with advanced stages of cirrhosis, which is in concordance with previous studies [46]. In fact, higher values of tyrosine have been associated with an increased mortality in patients with end-stage liver disease [47]. Moreover, methionine is a precursor of succinil-CoA, which is converted into succinic acid. In our study, lower succinic acid level was found with higher CTP scores. This fact seems to be in concordance with previous clinical trials that describe the succinate-containing infusion acts as hepatoprotective, promoting the transition from higher to lower values in the CTP score [48]. Moreover, p-cresol, a decreased metabolite in patients with higher CTP scores in our study, is produced from tyrosine by several bacteria. However, to our knowledge, there are no previous studies describing the level of these metabolites in HCV-related cirrhosis. Additionally, lower levels of BCAAs have been described in liver cirrhosis [49]. Ketoisocaproic acid is an intermediate in the leucine metabolism, with decreased levels as CTP increased, probably by its enhanced incorporation into proteins via enhancement of transamination to leucine [50]. This transamination is necessary to stimulate insulin secretion [51]. Besides, 2-keto-n-caproic acid (also called 2-ketohexanoic acid) is also a potent insulin secretagogue [52]. Therefore, since glucose metabolism is altered in HCV-infected patients [53] and insulin resistance is associated with hepatic fibrosis [54], the decreased level of BCAAs observed in our study could indicate a more damaged insulin and glucose metabolism in patients with higher CTP scores.

Carnitin, an amino acid derived naturally from lysine and methionine, plays a critical role in cellular energy production processes. Carnitin transfers long-chain fatty acids from cytosol into the mitochondrial for subsequent β-oxidation. Increased carnitine and acetylcarnitine levels have been described in patients with different types of cirrhosis, probably due to enhanced carnitine biosynthesis [55], showing an association independently of the cirrhosis aetiology [56]. However, to our knowledge, the association of these metabolites with advanced stages of cirrhosis in HIV/HCV-coinfected and HCV-monoinfected patients has not been described so far.

In our study, taurocholic acid was the metabolite that had the strongest positive association with the CTP score. Taurocholic acid has been described as the most changed bile acid in cirrhotic patients, mainly due to increased bile acid biosynthesis. It plays a crucial role in cirrhosis progression probably by the activation of the hepatic stellate cells (HSCs), being involved in the functional liver progenitor cells biliary differentiation with induction of chemokines that promote HSC recruitment [57]. Besides, taurocholic acid has been associated with hepatic inflammation and fibrosis, in addition to the induction of multiple pathways related to immune cells and cytokine signaling [58].

A similar trend in the association of individual metabolites for HIV/HCV-coinfected patients and HCV-monoinfected patients was observed, except for LPC(16:0) and LPC(18:0). However, the association strength was different, being higher in HIV/HCV coinfected patients. In the adjusted OLR model, all LPCs were significant for HIV/HCV-coinfected patients, with a protective role for liver disease. However, only LPC(20:3) and LPC(22:6) were significant and LPC(20:4) showed a trend in HCV-monoinfected patients, although significance was lost after controlling by multiple comparisons. This lack of significance is probably due to the more limited sample size in the HCV group, which could alter the ability to achieve statistically significant associations. According to our results, although it is well known that HIV infection promote inflammation, immune activation, oxidative stress and metabolic disorders, the effect of HIV infection on the metabolic profile in different stages of cirrhosis seems to be diluted by the advanced liver damage that suffer these patients. This could lead to the similar trend observed in both groups. Additionally, it is important to note as limitation that the multivariate models for studying the association of plasma metabolites with CTP for HIV/HCV and HCV groups could not be performed separately due to the limited sample size.

Glycolic acid, LPC(16:0) and taurocholic acid were the metabolites most significantly associated with decompensated cirrhosis (CTP score ≥7). When these three metabolites were combined together, they discriminated with great accuracy the presence of decompensated

cirrhosis, suggesting that could have an important role in the process of decompensation. They could be used as markers of decompensated cirrhosis; however further studies are needed among HCV-infected patients.

The limited sample size together with the low frequency of certain outcomes (e.g. treatment with statins, among others) could have limited the statistical power for some comparisons. Additionally, the limited sample size might also have increased the rate of false positives. However, positive findings were upheld with multiple testing correction, which gives robustness to our results.

Conclusions

In summary, altered plasma metabolomic profile was associated with advanced stages of cirrhosis in HIV/HCV-coinfected and HCV-monoinfected patients. Several metabolic processes changed with the advanced cirrhosis progression, including biosynthesis of fatty acids and phospholipids, cellular energy, oxidative stress, microbial fermentation, bile acids, insulin metabolism, and amino acid accumulation. Our findings contribute to a better understanding of the physiopathology of cirrhosis in HIV/HCV-coinfected and HCV-monoinfected patients.

References

1. WHO. Global Hepatitis Report. *World Health Organization* 2017.

2. Dietrich CG, Gotze O, Geier A. Molecular changes in hepatic metabolism and transport in cirrhosis and their functional importance. *World J Gastroenterol.* 2016;22(1):72-88.

3. Abutaleb A, Sherman KE. A changing paradigm: management and treatment of the HCV/HIV-co-infected patient. *Hepatol Int.* 2018;12(6):500-509.

4. Arroyo V, Garcia-Martinez R, Salvatella X. Human serum albumin, systemic inflammation, and cirrhosis. *J Hepatol.* 2014;61(2):396-407.

5. Schuppan D, Afdhal NH. Liver cirrhosis. *Lancet.* 2008;371(9615):838-851.

6. Peng Y, Qi X, Guo X. Child-Pugh Versus MELD Score for the Assessment of Prognosis in Liver Cirrhosis: A Systematic Review and Meta-Analysis of Observational Studies. *Medicine (Baltimore).* 2016;95(8):e2877.

7. Roche B, Coilly A, Duclos-Vallee JC, Samuel D. The impact of treatment of hepatitis C with DAAs on the occurrence of HCC. *Liver Int.* 2018;38 Suppl 1:139-145.

8. Berzigotti A. Advances and challenges in cirrhosis and portal hypertension. *BMC Med.* 2017;15(1):200.

9. Crouchet E, Lefevre M, Verrier ER, Oudot MA, Baumert TF, Schuster C. Extracellular lipid-free apolipoprotein E inhibits HCV replication and induces ABCG1-dependent cholesterol efflux. *Gut.* 2017;66(5):896-907.

10. Douglas DN, Pu CH, Lewis JT, et al. Oxidative Stress Attenuates Lipid Synthesis and Increases Mitochondrial Fatty Acid Oxidation in Hepatoma Cells Infected with Hepatitis C Virus. *J Biol Chem.* 2016;291(4):1974-1990.

11. Cassol E, Misra V, Holman A, Kamat A, Morgello S, Gabuzda D. Plasma metabolomics identifies lipid abnormalities linked to markers of inflammation, microbial translocation, and hepatic function in HIV patients receiving protease inhibitors. *BMC Infect Dis.* 2013;13:203.

12. Rodriguez-Gallego E, Gomez J, Pacheco YM, et al. A baseline metabolomic signature is associated with immunological CD4+ T-cell recovery after 36 months of antiretroviral therapy in HIV-infected patients. *AIDS.* 2018;32(5):565-573.

13. Binek A, Rojo D, Godzien J, et al. Flow Cytometry Has a Significant Impact on the Cellular Metabolome. *J Proteome Res.* 2019;18(1):169-181.

14. Kind T, Wohlgemuth G, Lee DY, et al. FiehnLib: mass spectral and retention index libraries for metabolomics based on quadrupole and time-of-flight gas chromatography/mass spectrometry. *Anal Chem.* 2009;81(24):10038-10048.

15. Gil-de-la-Fuente A, Godzien J, Saugar S, et al. CEU Mass Mediator 3.0: A Metabolite Annotation Tool. *J Proteome Res.* 2019;18(2):797-802.

16. Fiehn O, Robertson D, Griffin J, et al. The metabolomics standards initiative (MSI). *Metabolomics.* 2007;3(3):175-178.

17. Salek RM, Steinbeck C, Viant MR, Goodacre R, Dunn WB. The role of reporting standards for metabolite annotation and identification in metabolomic studies. *Gigascience.* 2013;2(1):13.

18. Langohr K, Sanvisens A, Fuster D, et al. Liver enzyme alterations in HCV-monoinfected and HCV/HIV-coinfected patients. *The open AIDS journal.* 2008;2:82-88.

19. Butorov EV. Plasma L-Carnitine and L-Lysine Concentrations in HIV-Infected Patients. *The open biochemistry journal.* 2017;11:119-131.

20. Schoeman JC, Moutloatse GP, Harms AC, et al. Fetal Metabolic Stress Disrupts Immune Homeostasis and Induces Proinflammatory Responses in Human Immunodeficiency Virus Type 1- and Combination Antiretroviral Therapy-Exposed Infants. *The Journal of infectious diseases.* 2017;216(4):436-446.

21. Zhou B, Lou B, Liu J, She J. Serum metabolite profiles as potential biochemical markers in young adults with community-acquired pneumonia cured by moxifloxacin therapy. *Sci Rep.* 2020;10(1):4436.

22. Rule JA, Hynan LS, Attar N, et al. Procalcitonin Identifies Cell Injury, Not Bacterial Infection, in Acute Liver Failure. *PLoS One.* 2015;10(9):e0138566.

23. Sidorov E, Sanghera DK, Vanamala JKP. Biomarker for Ischemic Stroke Using Metabolome: A Clinician Perspective. *J Stroke.* 2019;21(1):31-41.

24. Heimerl S, Fischer M, Baessler A, et al. Alterations of plasma lysophosphatidylcholine species in obesity and weight loss. *PLoS One.* 2014;9(10):e111348.

25. Diamanti K, Cavalli M, Pan G, et al. Intra- and inter-individual metabolic profiling highlights carnitine and lysophosphatidylcholine pathways as key molecular defects in type 2 diabetes. *Sci Rep.* 2019;9(1):9653.

26. Pleli T, Martin D, Kronenberger B, et al. Serum autotaxin is a parameter for the severity of liver cirrhosis and overall survival in patients with liver cirrhosis--a prospective cohort study. *PLoS One.* 2014;9(7):e103532.

27. Wu JM, Xu Y, Skill NJ, et al. Autotaxin expression and its connection with the TNF-alpha-NF-kappaB axis in human hepatocellular carcinoma. *Mol Cancer.* 2010;9:71.

28. Natarajan SK, Thomas S, Ramamoorthy P, et al. Oxidative stress in the development of liver cirrhosis: a comparison of two different experimental models. *J Gastroenterol Hepatol.* 2006;21(6):947-957.

29. Cichoz-Lach H, Michalak A. Oxidative stress as a crucial factor in liver diseases. *World J Gastroenterol.* 2014;20(25):8082-8091.

30. Sharma B. Oxidative stress in HIV patients receiving antiretroviral therapy. *Curr HIV Res.* 2014;12(1):13-21.

31. Arun P, Rittase WB, Wilder DM, Wang Y, Gist ID, Long JB. Defective methionine metabolism in the brain after repeated blast exposures might contribute to increased oxidative stress. *Neurochem Int.* 2018;112:234-238.

32. Jansson PJ, Jung HR, Lindqvist C, Nordstrom T. Oxidative decomposition of vitamin C in drinking water. *Free Radic Res.* 2004;38(8):855-860.

33. Ipson BR, Fisher AL. Roles of the tyrosine isomers meta-tyrosine and ortho-tyrosine in oxidative stress. *Ageing Res Rev.* 2016;27:93-107.

34. Copley SD, Frank E, Kirsch WM, Koch TH. Detection and possible origins of aminomalonic acid in protein hydrolysates. *Anal Biochem.* 1992;201(1):152-157.

35. van der Pol A, Gil A, Sillje HHW, et al. Accumulation of 5-oxoproline in myocardial dysfunction and the protective effects of OPLAH. *Sci Transl Med.* 2017;9(415).

36. Lupberger J, Croonenborghs T, Roca Suarez AA, et al. Combined Analysis of Metabolomes, Proteomes, and Transcriptomes of Hepatitis C Virus-Infected Cells and Liver to Identify Pathways Associated With Disease Development. *Gastroenterology.* 2019;157(2):537-551 e539.

37. Usami M, Miyoshi M, Yamashita H. Gut microbiota and host metabolism in liver cirrhosis. *World J Gastroenterol.* 2015;21(41):11597-11608.

38. Procopet B, Fischer P, Farcau O, Stefanescu H. Metabolomics: From liver chiromancy to personalized precision medicine in advanced chronic liver disease. *World J Hepatol.* 2018;10(3):371-378.

39. Gall WE, Beebe K, Lawton KA, et al. alpha-hydroxybutyrate is an early biomarker of insulin resistance and glucose intolerance in a nondiabetic population. *PLoS One.* 2010;5(5):e10883.

40. Newman JC, Verdin E. beta-hydroxybutyrate: much more than a metabolite. *Diabetes Res Clin Pract.* 2014;106(2):173-181.

41. Saibara T, Maeda T, Onishi S, Yamamoto Y. The arterial blood ketone body ratio as a possible marker of multi-organ failure in patients with alcoholic hepatitis. *Liver.* 1994;14(2):85-89.

42. Bialkowska AM. Strategies for efficient and economical 2,3-butanediol production: new trends in this field. *World J Microbiol Biotechnol.* 2016;32(12):200.

43. Cho EJ, Leem S, Kim SA, et al. Circulating Microbiota-Based Metagenomic Signature for Detection of Hepatocellular Carcinoma. *Sci Rep.* 2019;9(1):7536.

44. Li Y, Fu X, Ma X, et al. Intestinal Microbiome-Metabolome Responses to Essential Oils in Piglets. *Front Microbiol.* 2018;9:1988.

45. Wu Y, Wang M, Zhu Y, Lin S. Serum interleukin-6 in the diagnosis of bacterial infection in cirrhotic patients: A meta-analysis. *Medicine (Baltimore).* 2016;95(41):e5127.

46. Kakazu E, Kondo Y, Kogure T, et al. Plasma amino acids imbalance in cirrhotic patients disturbs the tricarboxylic acid cycle of dendritic cell. *Sci Rep.* 2013;3:3459.

47. Kinny-Koster B, Bartels M, Becker S, et al. Plasma Amino Acid Concentrations Predict Mortality in Patients with End-Stage Liver Disease. *PLoS One.* 2016;11(7):e0159205.

48. Gridchik IE, Kurdyakov AV, Matveev AI. [Experience in Use of Hepatoprotector Remaxol for Treating Liver Cirrhosis]. *Eksp Klin Farmakol.* 2015;78(12):11-14.

49. Blonde-Cynober F, Aussel C, Cynober L. Abnormalities in branched-chain amino acid metabolism in cirrhosis: influence of hormonal and nutritional factors and directions for future research. *Clin Nutr.* 1999;18(1):5-13.

50. Blonde-Cynober F, Plassart F, de Bandt JP, et al. Metabolism of alpha-ketoisocaproic acid in isolated perfused liver of cirrhotic rats. *Am J Physiol.* 1995;268(2 Pt 1):E298-304.

51. Zhou Y, Jetton TL, Goshorn S, Lynch CJ, She P. Transamination is required for {alpha}-ketoisocaproate but not leucine to stimulate insulin secretion. *J Biol Chem.* 2010;285(44):33718-33726.

52. Lenzen S, Formanek H, Panten U. Signal function of metabolism of neutral amino acids and 2-keto acids for initiation of insulin secretion. *J Biol Chem.* 1982;257(12):6631-6633.

53. Vespasiani-Gentilucci U, Gallo P, De Vincentis A, Galati G, Picardi A. Hepatitis C virus and metabolic disorder interactions towards liver damage and atherosclerosis. *World J Gastroenterol.* 2014;20(11):2825-2838.

54. Patel S, Jinjuvadia R, Patel R, Liangpunsakul S. Insulin Resistance is Associated With Significant Liver Fibrosis in Chronic Hepatitis C Patients: A Systemic Review and Meta-Analysis. *J Clin Gastroenterol.* 2016;50(1):80-84.

55. Krahenbuhl S, Reichen J. Carnitine metabolism in patients with chronic liver disease. *Hepatology.* 1997;25(1):148-153.

56. Amodio P, Angeli P, Merkel C, Menon F, Gatta A. Plasma carnitine levels in liver cirrhosis: relationship with nutritional status and liver damage. *J Clin Chem Clin Biochem.* 1990;28(9):619-626.

57. Pozniak KN, Pearen MA, Pereira TN, et al. Taurocholate Induces Biliary Differentiation of Liver Progenitor Cells Causing Hepatic Stellate Cell Chemotaxis in the Ductular Reaction: Role in Pediatric Cystic Fibrosis Liver Disease. *Am J Pathol.* 2017;187(12):2744-2757.

58. Janssen AWF, Houben T, Katiraei S, et al. Modulation of the gut microbiota impacts nonalcoholic fatty liver disease: a potential role for bile acids. *J Lipid Res.* 2017;58(7):1399-1416.

Figure legends

Figure 1. Multivariate analysis for cirrhosis progression according to CTP score, in HIV/HCV and HCV infected patients. A) PLS-DA plot resulting from GC-MS data and metabolites with the highest VIP score (≥1); B) PLS-DA resulting from LC-MS ESI+ data and metabolites with the highest VIP score (≥1).

Statistics: Multivariate analysis was performed by partial least squares discriminant analysis (PLS-DA). The VIP score measures the variable's importance and allows metabolites to be ranked according to their importance.

Abbreviations: GC-MS, gas chromatography–mass spectrometry; LC-MS, and liquid chromatography–mass spectrometry; ESI, electrospray ionization; PC, phosphatidylcholine; LPC, lysophosphatidylcholine; LPE, lysophosphatidylethanolamine.

Figure 2. Association of significant metabolites resulting from univariate analysis with the CTP score, stratifying by HIV coinfection.

Statistics: Adjusted odd ratio (aOR) and 95% of confidence interval (95%CI) were calculated by ordinal regression models adjusted by the main baseline characteristics of patients (see Statistical analysis in Patients and methods section). *P*-values were adjusted by FDR correction for multiple comparisons (Benjamini and Hochberg).

Abbreviations: HIV, human immunodeficiency virus; HCV, hepatitis C virus; LPC, lysophosphatidylcholine; LPC, lysophosphatidylcholine; LPE, lysophosphatidylethanolamine.

Figure 3. ROC curves of plasma biomarkers for predicting decompensated cirrhosis in patients with advanced HCV-related cirrhosis.

Statistics: Values were expressed as area under the receiver operating characteristic (AUROC) and 95% confidence interval (95%CI).

Abbreviations: ROC, receiver operating characteristic; AUC-ROC, area under the curve ROC; CI, confidence interval; LPC, lysophosphatidylcholine; p, level of significance.

Figure 4. Heatmap of metabolites significantly related to the progression of advanced cirrhosis (distance measure using Euclidean, clustering algorithm using ward). Score 5, 6, 7 and 8 of CTP are represented by columns.

Additional Files

File name: Additional File 1.

Format: .docx

Title and description of data: Additional description of methods section.

File name: Additional File 2.

Format: .tif

Title and description of data: Principal component analysis (PCA) plot showing clustering of study samples and quality controls. **Abbreviations:** GC-MS, gas chromatography–mass spectrometry; LC-MS, and liquid chromatography–mass spectrometry; ESI, electrospray ionization; PC, principal component.

File name: Additional File 3.

Format: .tif

Title and description of data: Multivariate analysis of plasma metabolites regarding HIV coinfection. PLS-DA plot resulting from GC-MS data and metabolites with the highest VIP score (≥1). **Statistics**: Multivariate analysis was performed by partial least squares discriminant analysis (PLS-DA). The VIP score measures the variable's importance and allows metabolites to be ranked according to their importance. **Abbreviations**: PLS-DA, partial least squares discriminant analysis, VIP, variable importance in projection, GC-MS, gas chromatography–mass spectrometry.

File name: Additional File 4.

Format: .docx

Title and description of data: Summary of associations between metabolites and HIV coinfection (HCV/HIV coinfected vs. HCV monoinfected patients). **Statistics:** Values are expressed as odds ratio and 95% confidence interval. P-values were calculated by GLM with binomial distribution (logit-link); q-values represent p-values corrected for multiple testing using the false discovery rate (FDR). Adjusted models were adjusted by the most significant

clinical and epidemiological characteristics (see Statistical analysis section). Statistically significant differences are shown in bold. **Abbreviations**: OR, odds ratio; aOR, adjusted odds ratio; 95%CI, 95% of confidence interval; p-value, level of significance; q-value, corrected level of significance; PC, phosphatidylcholine; LPC, lysophosphatidylcholine.

File name: Additional File 5.

Format: .tif

Title and description of data: Multivariate analysis of plasma metabolites regarding high alcohol intake (>50 g/day). PLS-DA plot resulting from GC-MS data and metabolites with the highest VIP score (≥1). **Statistics:** Multivariate analysis was performed by PLS-DA. The VIP score measures the variable's importance and allows metabolites to be ranked according to their importance. **Abbreviations**: PLS-DA, partial least squares discriminant analysis, VIP, variable importance in projection, GC-MS, gas chromatography–mass spectrometry.

File name: Additional File 6.

Format: .docx

Title and description of data: Summary of associations between plasma metabolites and high alcohol intake (>50 g/day). **Statistics:** Values are expressed as odds ratio and 95% confidence interval. P-values were calculated by ordinal logistic regression analysis; q-values represent p-values corrected for multiple testing using the false discovery rate (FDR). Adjusted models were adjusted by the most significant clinical and epidemiological characteristics (see Statistical analysis section). Statistically significant differences are shown in bold. **Abbreviations**: OR, odds ratio; aOR, adjusted odds ratio; 95%CI, 95% of confidence interval; p-value, level of significance; q-value, corrected level of significance.

File name: Additional File 7.

Format: .docx

Title and description of data: Summary of associations between metabolites and previous HCV therapy failure. **Statistics:** Values are expressed as odds *ratio* and 95% confidence interval. P-values were calculated by GLM model with binomial distribution; q-values represent p-values corrected for multiple testing using the false discovery rate (FDR).

Adjusted models were adjusted by the most significant clinical and epidemiological characteristics (see Statistical analysis section). Statistically significant differences are shown in bold. **Abbreviations**: OR, odds ratio; aOR, adjusted odds ratio; 95%CI, 95% of confidence interval; p-value, level of significance; q-value, corrected level of significance.

File name: Additional File 8.

Format: .tif

Title and description of data: Permutation by separation distance (B/W) to confirm the validity of the PLS-DA models, with a permutation number of 1000. **Abbreviations:** GC-MS, gas chromatography–mass spectrometry; LC-MS, and liquid chromatography–mass spectrometry; ESI, electrospray ionization.

File name: Additional File 9.

Format: .docx

Title and description of data: Summary of the highest variable importance in projection (VIP) scores for the multivariate analysis of metabolites according to the CTP score. **Statistics:** Partial least squares discriminant analysis (PLS-DA) was used to calculate the VIP score for each of the metabolites. The VIP score measures the variable's importance and allows ranking of the metabolites according to their importance. **Abbreviations:** GC-MS, gas chromatography–mass spectrometry; LC-MS, and liquid chromatography–mass spectrometry; ESI, electrospray ionization; PC, phosphatidylcholine; LPC, lysophosphatidylcholine; LPE, lysophosphatidylethanolamine.

File name: Additional File 10.

Format: .docx

Title and description of data: Association between individual metabolites and CTP score. **Statistics:** A) Significant metabolites from unadjusted ordinal regression models (dependent variable: CTP score; independent variable: metabolites); B) Significant metabolites from ordinal regression models (dependent variable: CTP score; independent variable: metabolites) adjusted by the most relevant covariates (see Statistical analysis in Patients and methods section). *P*-values were adjusted by FDR correction for multiple comparisons

(Benjamini and Hochberg). **Abbreviation**s: RT, retention time; OR, odd ratio; CI, confidence interval; p-value, level of significance; q-value, adjusted p-value by FDR correction; LPC, lysophosphatidylcholine.

File name: Additional File 11.

Format: .docx

Title and description of data: Summary of unadjusted and adjusted associations between plasma metabolites and hepatic decompensation (CTP ≥7). **Statistics:** Values are expressed as odds ratio and 95% confidence interval. P-values were calculated by GLM model with binomial distribution; q-values represent p-values corrected for multiple testing using the false discovery rate (FDR). Adjusted models were adjusted by the most significant clinical and epidemiological characteristics (see Statistical analysis section). Statistically significant differences are shown in bold. **Abbreviations**: OR, odds ratio; aOR, adjusted odds ratio; 95%CI, 95% of confidence interval; p-value, level of significance; q-value, corrected level of significance; LPC, lysophosphatidylcholine; LPE, lysophosphatidylethanolamine.

File name: Additional File 12.

Format: .docx

Title and description of data: Correlation between bacteria-related metabolites and bacterial translocation and infection. **Statistics:** *P*-values were calculated by Spearman correlation. Statistically significant differences are shown in bold. **Abbreviations**: r, Spearman correlation coefficient; p, level of significance; LPS, lipopolysaccharide; LBP, lipopolysaccharide binding protein; IL6, interleukin 6.

Appendix

The ESCORIAL study group.

Hospital General Universitario Gregorio Marañón (Madrid, Spain): Cristina Díez, Luis Ibáñez, Leire Pérez-Latorre, Diego Rincón, Teresa Aldámiz-Echevarría, Vega Catalina, Pilar Miralles, Teresa Aldámiz-Echevarría, Francisco Tejerina, María C Gómez-Rico, Esther Alonso, José M Bellón, Rafael Bañares, and Juan Berenguer.

Hospital Universitario La Paz/IdiPAZ (Madrid, Spain): José Arribas, José I Bernardino, Carmen Busca, Javier García-Samaniego, Víctor Hontañón, Luz Martín-Carbonero, Rafael Micán, María L Montes-Ramírez, Victoria Moreno, Antonio Olveira, Ignacio Pérez-Valero, Eulalia valencia, and Juan González-García.

Hospital Universitario Puerta de Hierro (Madrid, Spain): Elba Llop and José Luis Calleja.

Hospital Universitario Ramón y Cajal (Madrid, Spain): Javier Martínez and Agustín Albillos.

Fundación SEIMC/GeSIDA (Madrid, Spain): Marta de Miguel, María Yllescas, and Herminia Esteban.

Table 1. Clinical and epidemiological characteristics of patients with advanced HCV-related cirrhosis according to Child-Pugh-Turcotte score.

		Child-Pugh-Turcotte strata				
	All patients	**Score 5**	**Score 6**	**Score 7**	**Score 8**	***p***
No.	90	63	14	8	5	-
Age (years)	52.9 (48.9-56.4)	53.1 (50.5-56.5)	52.9 (48.9-54.6)	50 (45.7-57.9)	52.1 (48.8-53.8)	0.786
Gender (male)	63 (70.0%)	43 (68.3%)	8 (57.1%)	8 (100.0%)	4 (80.0%)	0.182
BMI (kg/m^2)	24.5 (22.4-27.7)	24.1 (22.1-27.4)	25.6 (21.7-31.2)	25.6 (23.3-26.9)	27.3 (25.0-28.4)	0.490
Smoker (n=89)						
Never	17 (19.1%)	13 (21.0%)	3 (21.4%)	1 (12.5%)	0 (0.0%)	0.108
Previously (≥ 6 months)	22 (24.7%)	15 (24.2%)	2 (14.3%)	1 (12.5%)	4 (80.0%)	
Nowadays	50 (56.2%)	34 (54.8%)	9 (64.3%)	6 (75.0%)	1 (20.0%)	
Alcohol intake (>50 g/day)						
Never	44 (48.9%)	33 (52.4%)	6 (42.9%)	3 (37.5%)	3 (60.0%)	0.421
Previously (≥ 6 months)	38 (42.2%)	24 (38.1%)	8 (57.1%)	3 (37.5%)	3 (60.0%)	
Nowadays	8 (8.9%)	6 (9.5%)	0 (0%)	2 (25.0%)	0 (0%)	
IVDP	53 (58.9%)	39 (61.9%)	6 (42.9%)	5 (62.5%)	3 (60.0%)	0.622
Previous anti-HCVtherapy	44 (48.9%)	31 (49.2%)	6 (42.9%)	4 (50.0%)	3 (60.0%)	0.928
Treatment with statins	9 (10%)	8 (12.7%)	1 (7.1%)	0 (0.0%)	0 (0.0%)	0.556
Other liver markers						
MELD	9 (8-11)	8 (7-10)	10 (9-12)	12 (11-13)	13 (11-13)	**<0.001**
LSM	30.4 (23.6-41.6)	27.4 (21.3-36.3)	43.5 (21.5-49.6)	36.1 (28.1-45.8)	47.2 (35.3-52.2)	**0.028**
HVPG	15.5 (13.0-18.0)	14.3 (10.0-17.0)	17.0 (15.5-21.0)	17.0 (16.0-18.0)	18.5 (18.0-20.0)	**0.008**
Ascites	27 (30.0%)	16 (25.4%)	5 (35.7%)	4 (50.0%)	2 (40.0%)	0.455
Bleeding esophageal varices	8 (8.9%)	6 (9.5%)	1 (7.1%)	1 (12.5%)	0 (0%)	0.873
Hepatic encephalopathy	8 (9.0%)	7 (11.3%)	0 (0%)	1 (12.5%)	0 (0%)	0.494
Carcinoma hepatocellular	1 (1.1%)	1 (1.6%)	0 (0%)	0 (0%)	0 (0%)	0.932
HCV markers						

HCV genotype (n=88)						
1	60 (68.2%)	41 (65.1%)	12 (85.7)	3 (50.0%)	4 (80.0%)	**0.041**
2	1 (1.1%)	0 (0%)	0 (0%)	1 (16.7%)	0 (0%)	
3	12 (13.6%)	9 (14.3%)	1 (7.1%)	1 (16.7%)	1 (20.0%)	
4	15 (17.0%)	13 (20.6%)	1 (7.1%)	1 (16.7%)	0 (0%)	
Log_{10} HCV-RNA (IU/mL) (n=89)	6.2 (5.5-6.6)	6.3 (5.8-6.7)	5.8 (5.4-6.3)	5.5 (5.2-5.9)	6.2 (5.2-6.2)	0.059
HCV-RNA > 850,000 IU/mL (n=89)	55 (61.8%)	18 (29.0%)	6 (42.9%)	2 (25.0%)	3 (60.0%)	**0.030**
HIV markers						
HIV coinfection	62 (68.9%)	48 (76.2%)	9 (64.3%)	3 (37.5%)	2 (40.0%)	0.062
Previous AIDS (n=62)	21 (33.9%)	15 (31.3%)	4 (44.4%)	1 (33.3%)	1 (50.0%)	0.842
Nadir $CD4^+$ T cells (n=57)	130 (70-242)	110.4 (54.0-223.0)	130 (72.0-247.0)	300 (99-478)	175.5 (144-207)	0.388
Nadir $CD4^+$ T cells<200 cells/mm^3 (n=57)	38 (66.7%)	31 (72.1%)	5 (55.6%)	1 (33.3%)	1 (50%)	0.420
Baseline $CD4^+$ T cells (n=62)	447 (234-719)	452 (238-722)	444 (372-558)	378 (150-685)	439 (164-714)	0.897
Baseline $CD4^+$ T cells<500 cells/mm^3 (n=62)	36 (58.1%)	28 (58.3%)	5 (55.6%)	2 (66.7%)	1 (50.0%)	0.982
Antiretroviral therapy (n=61)						
NRTI+NNRTI	7 (11.5%)	5 (10.4%)	2 (25%)	0 (0%)	0 (0%)	0.426
NRTI+II	34 (55.7%)	28 (58.3%)	3 (37.5%)	2 (66.7%)	1 (50.0%)	
NRTI+PI	6 (9.8%)	6 (12.5%)	0 (0%)	0 (0%)	0 (0%)	
PI+II+NNRTI/MVC	4 (6.6%)	2 (4.2%)	1 (12.5%)	0 (0%)	1 (50.0%)	
Others	10 (16.4%)	7 (14.6%)	2 (25%)	1 (33.3%)	0 (0%)	

Statistics: Values expressed as absolute number (percentage) and median (interquartile range). *P*-values were calculated by Chi-square tests and Mann-Whitney tests. **Abbreviations**: BMI, body mass index; IVDU, intravenous drug user; HCV, hepatitis C virus; HCV-RNA, HCV plasma viral load; HIV, human immunodeficiency; MELD, model for end-stage liver disease; LSM, liver stiffness measurement; HVPG, hepatic venous pressure gradient; AIDS, acquired immune deficiency syndrome; NNRTI, non-nucleoside analogue HIV reverse transcriptase inhibitor; NRTI, nucleoside analogue HIV reverse transcriptase inhibitor; PI, protease inhibitor; II, integrase inhibitor, MVC, maraviroc.

Table 2. Summary of associations between metabolites and the Child-Pugh-Turcotte score.

		Unadjusted model			Adjusted model		
Metabolite	**Technology**	**OR (95%CI)**	**p-value**	**q-value**	**aOR (95%CI)**	**p-value**	**q-value**
Glycolic acid	GC-MS	2.35 (1.44-3.98)	0.001	0.058	2.66 (1.56; 4.87)	6.8×10^{-4}	**0.001**
LPC(20:3)	LC-MS ESI+	0.45 (0,25-0,75)	0.004	0.082	0.36 (0.18-0.65)	0.001	**0.002**
LPC(18:0)	LC-MS ESI+	0.47 (0.28-0.76)	0.003	0.072	0.42 (0.24-0.70)	0.001	**0.002**
LPC(16:0)	LC-MS ESI+	0.37 (0.21-0.63)	$4.7*10^{-4}$	**0.027**	0.32 (0.16-0.59)	4.8×10^{-4}	**0.001**
LPC(20:4)	LC-MS ESI+	0.39 (0.21-0.67)	0.001	**0.044**	0.39 (0.21-0.69)	0.002	**0.003**
LPC(22:6)	LC-MS ESI+	0.44 (0.25-0.73)	0.002	0.064	0.32 (0.17-0.57)	2.4×10^{-4}	**0.001**
LPE (22:6)	LC-MS ESI+	0.48 (0.29-0.76)	0.003	0.067	0.46 (0.26-0.78)	0.005	**0.006**
Taurocholic acid	LC-MS ESI-	2.63 (1.58-4.65)	$4.1*10^{-4}$	0.084	3.62 (1.96-7.30)	1.1×10^{-4}	**0.001**

Statistics: Values are expressed as odds ratio and 95% confidence interval. P-values were calculated by ordinal logistic regression analysis; q-values represent p-values corrected for multiple testing using the false discovery rate (FDR). Adjusted models were adjusted by the most significant clinical and epidemiological characteristics (see Statistical analysis section). Statistically significant differences are shown in bold.
Abbreviations: OR, odds ratio; aOR, adjusted odds ratio; 95%CI, 95% of confidence interval; p-value, level of significance; q-value, corrected level of significance; LPC, lysophosphatidylcholine; LPE, lysophosphatidylethanolamine.

A) GC-MS

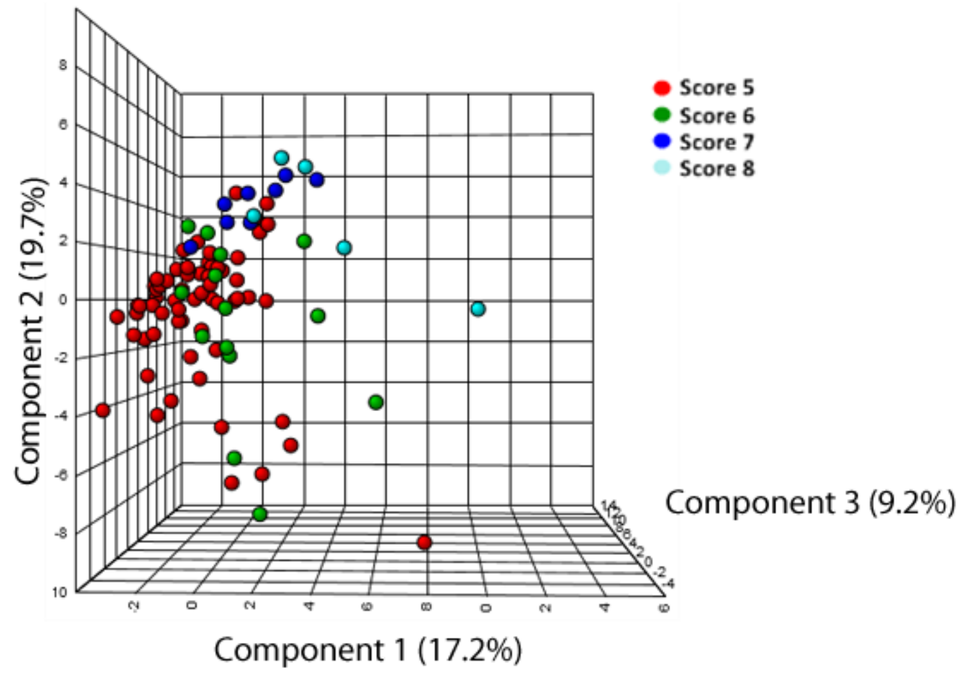

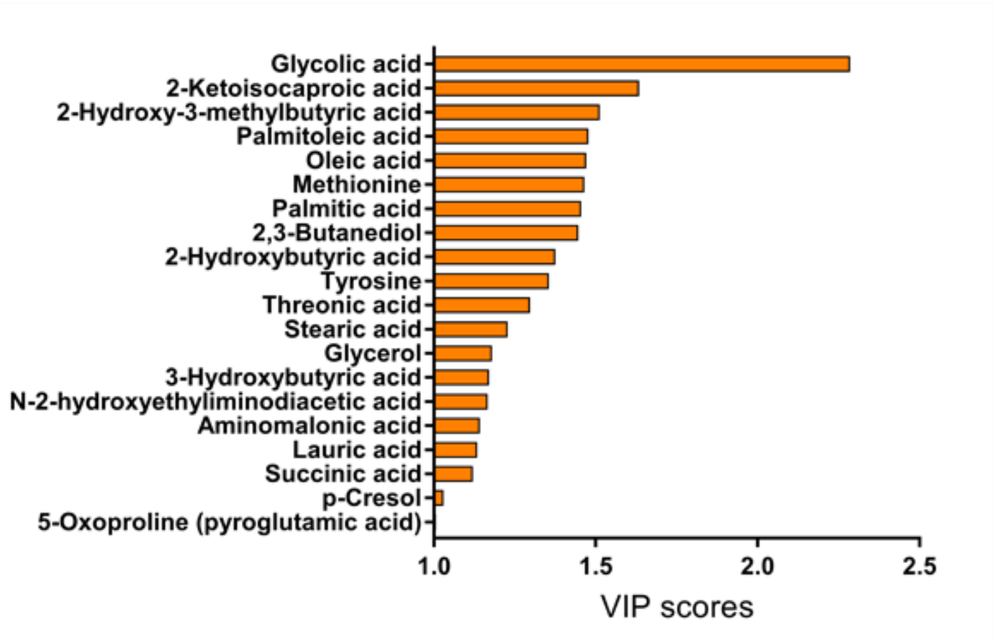

B) LC-MS ESI+

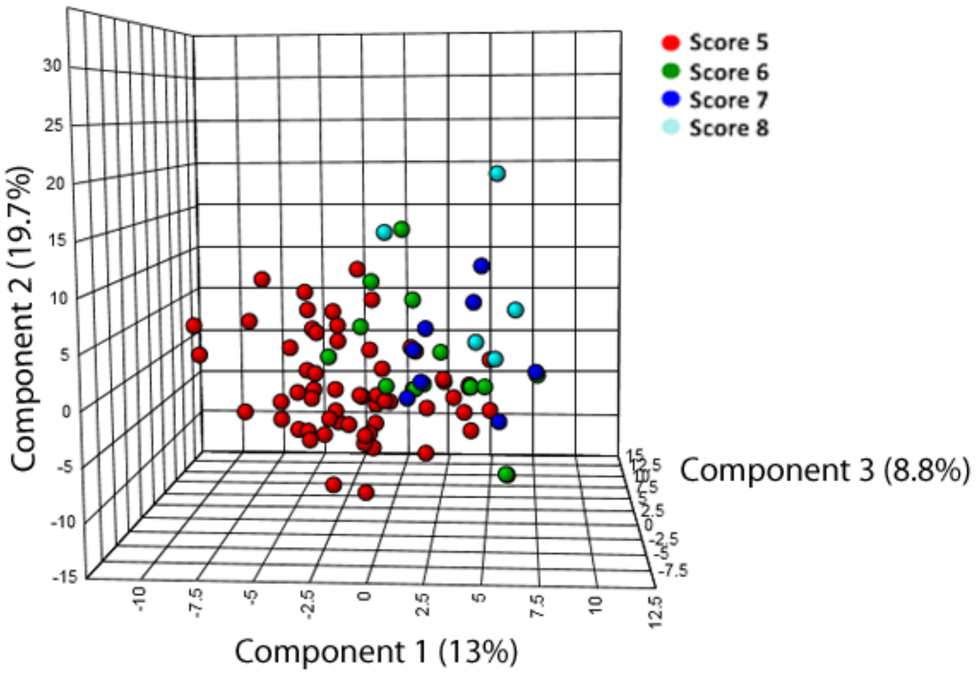

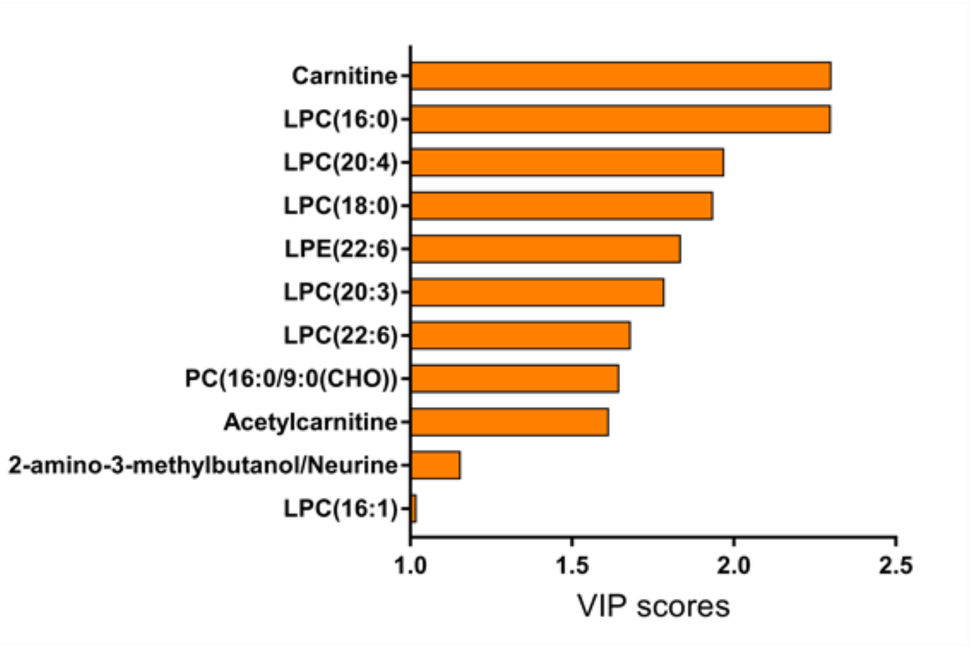

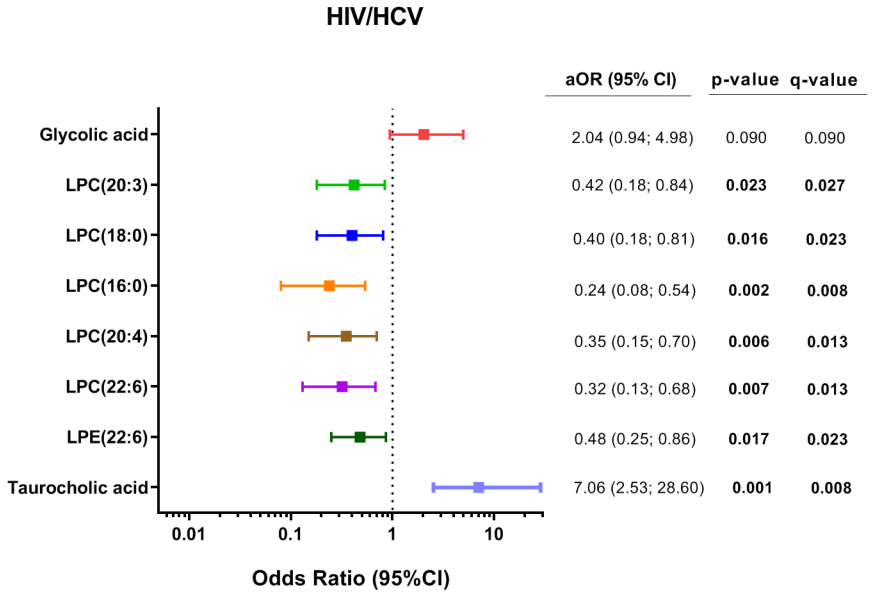
HIV/HCV
aOR (95% CI)
p-value
q-value
Glycolic acid
2.04 (0.94; 4.98)
0.090
0.090
LPC(20:3)
0.42 (0.18; 0.84)
0.023
0.027
LPC(18:0)
0.40 (0.18; 0.81)
0.016
0.023
LPC(16:0)
0.24 (0.08; 0.54)
0.002
0.008
LPC(20:4)
0.35 (0.15; 0.70)
0.006
0.013
LPC(22:6)
0.32 (0.13; 0.68)
0.007
0.013
LPE(22:6)
0.48 (0.25; 0.86)
0.017
0.023
Taurocholic acid
7.06 (2.53; 28.60)
0.001
0.008
0.01
0.1
1
10
Odds Ratio (95%CI)

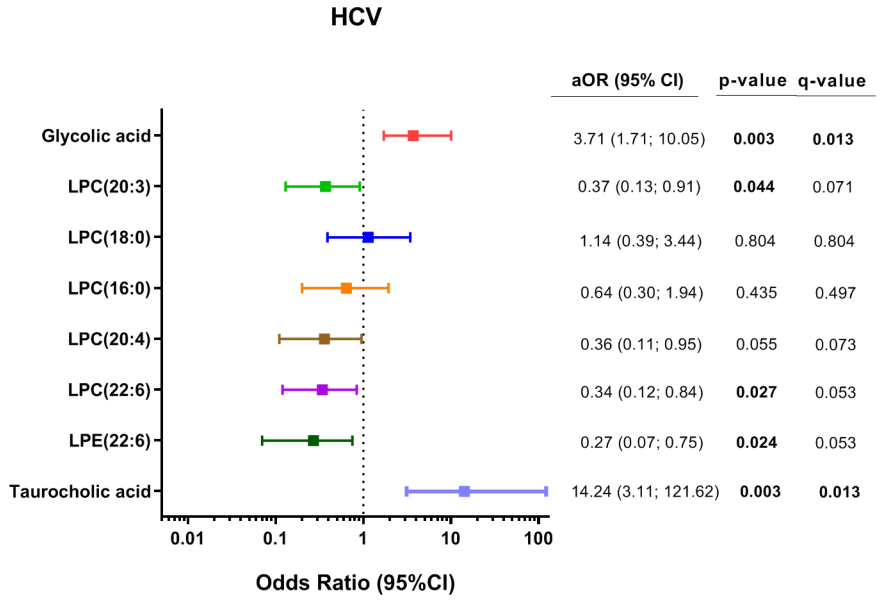
HCV
aOR (95% CI)
p-value
q-value
Glycolic acid
3.71 (1.71; 10.05)
0.003
0.013
LPC(20:3)
0.37 (0.13; 0.91)
0.044
0.071
LPC(18:0)
1.14 (0.39; 3.44)
0.804
0.804
LPC(16:0)
0.64 (0.30; 1.94)
0.435
0.497
LPC(20:4)
0.36 (0.11; 0.95)
0.055
0.073
LPC(22:6)
0.34 (0.12; 0.84)
0.027
0.053
LPE(22:6)
0.27 (0.07; 0.75)
0.024
0.053
Taurocholic acid
14.24 (3.11; 121.62)
0.003
0.013
0.01
0.1
1
10
100
Odds Ratio (95%CI)

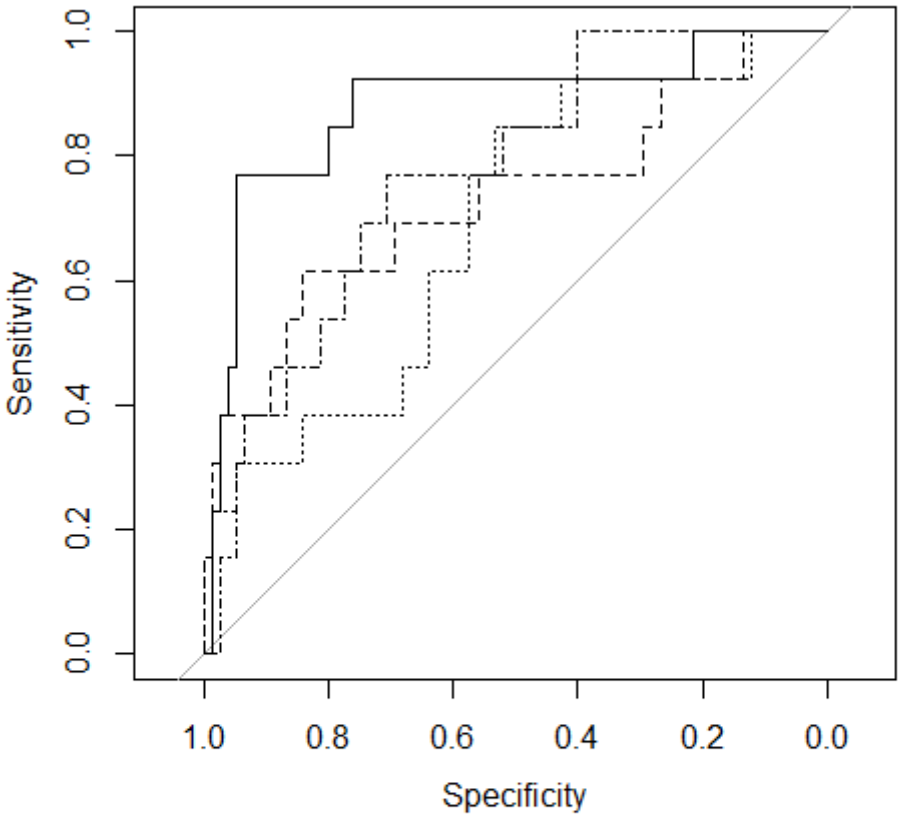

	Metabolite	AUC-ROC (95% CI)	*p*
———	Glycolic acid + LPC(16:0) + Taurocholic acid	0.879 (0.757-1.000)	REF
- - - - -	Glycolic acid	0.730 (0.554-0.907)	0.012
·····	LPC(16:0)	0.689 (0.534-0.845)	0.009
-·-·-·-	Taurocholic acid	0.769 (0.641-0.897)	0.175

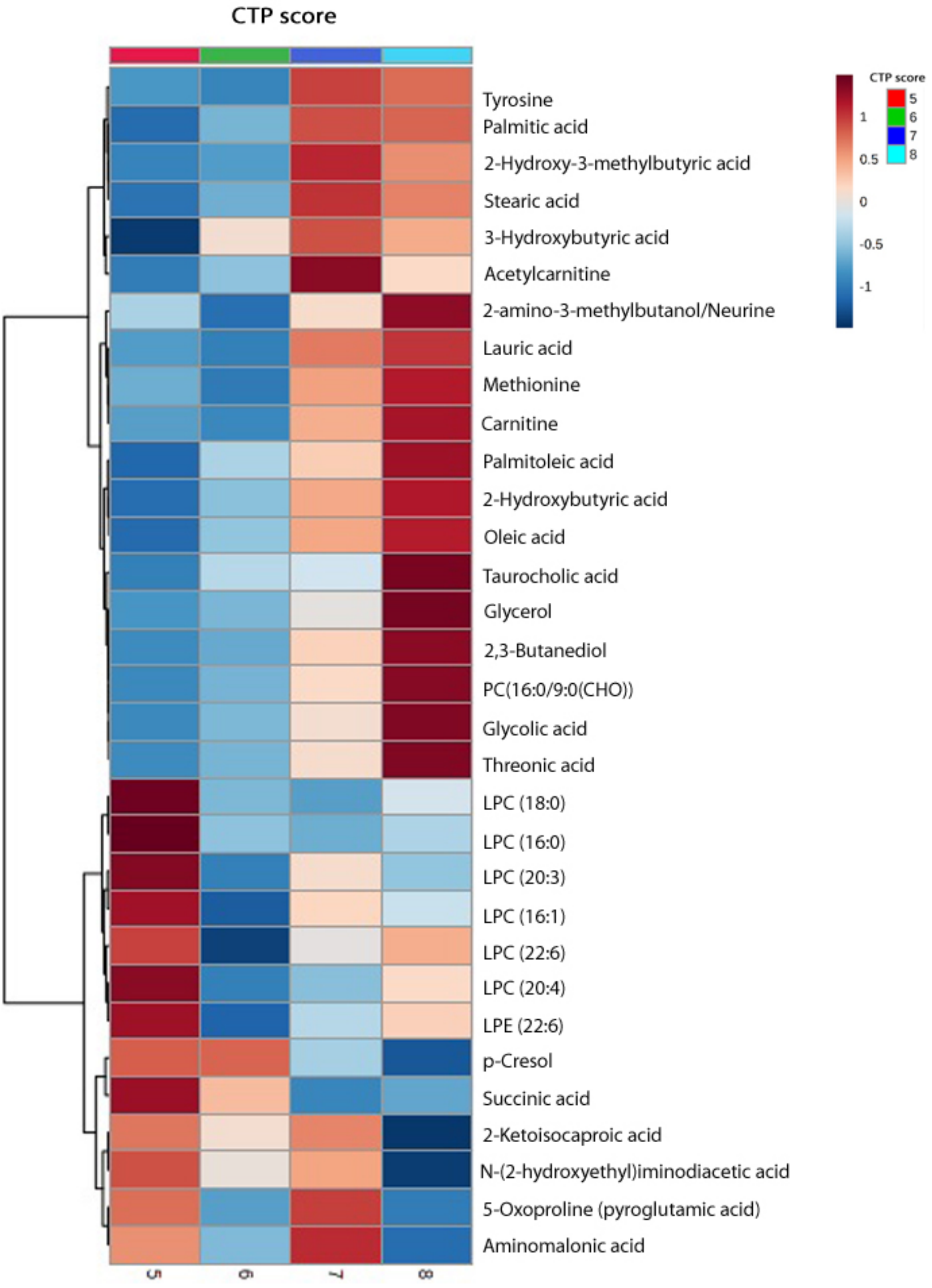
CTP score
Tyrosine
Palmitic acid
2-Hydroxy-3-methylbutyric acid
Stearic acid
3-Hydroxybutyric acid
Acetylcarnitine
2-amino-3-methylbutanol/Neurine
Lauric acid
Methionine
Carnitine
Palmitoleic acid
2-Hydroxybutyric acid
Oleic acid
Taurocholic acid
Glycerol
2,3-Butanediol
PC(16:0/9:0(CHO))
Glycolic acid
Threonic acid
LPC (18:0)
LPC (16:0)
LPC (20:3)
LPC (16:1)
LPC (22:6)
LPC (20:4)
LPE (22:6)
p-Cresol
Succinic acid
2-Ketoisocaproic acid
N-(2-hydroxyethyl)iminodiacetic acid
5-Oxoproline (pyroglutamic acid)
Aminomalonic acid
5
6
7
8
CTP score
1
0.5
0
-0.5
-1

Additional File 1: Additional description of methods section.

Reagents and standards for metabolomics

They have been used: acetonitrile (LC-MS grade, Sigma-Aldrich, Steinheim, Germany), formic acid (FA) (MS grade, Sigma-Aldrich, Steinheim, Germany), MilliQ® water (Millipore, Billerica, MA, USA), heptane (Sigma-Aldrich, Steinheim, Germany), methylterbutyleter (MTBE) (Sigma-Aldrich, Steinheim, Germany), pyridine (Sigma-Aldrich, Steinheim, Germany), O-methoxyamine hydrochloride (Sigma-Aldrich, Steinheim, Germany) and N,O-bis(trimethylsilyl) trifluoroacetamide (BSTFA) plus 1 % trimethylchlorosilane (TMCS) (Pierce Chemical Co, Rockford, IL, USA). Stearic acid methyl ester (C18:0 methyl ester) (Sigma-Aldrich, Steinheim, Germany) was used as internal standard for GC-MS. For reference masses purine, hexakis(1H,1H,3H-tetrafluoropropoxy)phosphazine (HP) and ammonium trifluoroacetate (TFA(NH_4)) from Agilent (API-TOF reference mass solution kit) were used in LC-MS. In GC-MS, a FAME mix (fatty acid methyl esters, e.g. caprylic acid, capric acid, lauric acid, tridecanoic acid, myristic acid, myristoleic acid, pentadecanoic acid, palmitic acid, palmitoleic acid, heptadecanoid acid, stearic acid, elaidic acid, oleic acid, linoleic acid, arachidic acid, cis-11-eicosenoic acid, linolenic acid, behenic acid and erucic acid) was purchased from Supelco (Bellefonte, PA, USA).

Sample preparation for metabolomics analysis

In the day of the analysis, for GC-MS 100 µL of the corresponding methanolic aliquots were evaporated to dryness using a Speedvac Concentrator, followed by the addition of 10 µL of O-methoxyamine hydrochloride (15 mg/mL) in pyridine for methoximation. After gently vortexing, the vials were incubated in darkness at room temperature for 16 hours. Then, 10 µL of BSTFA with 1 % TMCS (v/v) were added and samples were vortexed for 5 min, silylation was carried out for 1 h at 70°C and finally 100 µL of C18:0 methyl ester (10 mg/L in heptane) were added as an internal standard and samples were mixed again by gently vortex. Six blank samples were prepared by the same procedure of extraction and derivatization. For LC-MS, 500 µL of MTBE were added to the samples to enhance the extraction of the lipophilic compounds. After gently vortexing (TissueLyser LT, 50 Hz, 10 min) and centrifugation (16000 g, 20 min, 4°C), the resulting supernatants were filtered

through 0.22 µm nylon syringe filters and transferred into an analytical vial for their analysis.

Quality controls (QCs) samples are required at the beginning of the sequence to stabilize the system and throughout the analytical runs at periodic intervals of time to monitor variations in signal across the time. For these reasons, individual QC samples were prepared independently for each analytical platform by pooling and mixing equal volumes of each corresponding sample. After gently vortex, the mixes were transferred to analytical vials.

GC-EI-Q-MS fingerprinting (for using FiehnLib [1] and NIST 14 libraries)

GC system (Agilent Technologies 7890A) consisted in an autosampler (Agilent Technologies 7693) and an inert mass selective detector (MSD) with Quadrupole (Agilent Technologies 5975). Two µL of the derivatized sample were injected through a GC-Column DB5-MS (30 m length, 0.25 mm internal diameter, 0.25 µm film 95% dimethylpolysiloxane / 5% diphenylpolysiloxane) with a pre-column (10 m J&W integrated with Agilent 122-5532G). The flow rate of the helium carrier gas was set at 1 mL/min and the injector temperature 250°C. The split ratio was 1:10 flow into a Restek 20782 deactivated glass-wool split liner. The temperature gradient was programmed at 60°C (held for 1 min), with a ramping increase rate of 10 °C/min up to 325°C. Finally, it was cooled down for 10 min before the next injection. The total analysis time was 37.5 min. The detector transfer line, filament source and quadrupole temperature were respectively set at 290°C, 230°C and 150°C. The electron ionization (EI) source was placed at 70 eV. The mass spectrometer operated in scan mode over a mass range of *m/z* 50–600 at a rate of 2 spectra per second. The method was retention time locked at 19.663 minutes (elution time of the internal standard). The analytical run was set up starting with the injection of C18:0 methyl ester (10 mg/L in heptane) and FAME mix (0.1 mg/mL in CH_2Cl_2) followed by four blanks, five QCs and then samples were analysed in a randomised order, where other QCs were injected between blocks of ten samples until the end of the run that terminated with the injection of the four blanks.

LC-ESI-QTOF-MS fingerprinting

The metabolic profile was achieved using a liquid chromatography system consisting of a degasser, a binary pump, and an autosampler (1290 infinity II,

Agilent). Samples (0.5 µL) were applied to a reversed-phase column (Zorbax Extend C18 50 x 2.1 mm, 1.8 µm; Agilent), which was maintained at 60°C during the analysis. The system was operated at a flow rate of 0.6 mL/min with solvent A (H_2O containing 0.1% FA) and solvent B (acetonitrile containing 0.1% FA). The gradient was 5% B (0–1 min), 5 to 80% B (1–7 min), 80 to 100% B (7–11.5 min), and 100 to 5% B (11.5–12 min). The system was finally held at 5% B for 3 min to re-equilibrate the system (15 min of total analysis time). Data were collected in positive and negative electrospray ionization (ESI) modes in separate runs using QTOF (Agilent 6550 iFunnel). The analyses were performed in both positive and negative ion modes in full-scan from *m/z* 50 to 1000. The capillary voltage was 3000 V and the nozzle voltage was 1000 V with a scan rate of 1.0 spectrum per second. The gas temperature was 250°C, the drying gas flow was 12 L/min, the nebulizer was 52 psi, the sheath gas temperature 370°C and the sheath gas flow 11 L/min. For positive mode, the MS-TOF parameters were as follows: fragmentor 175 V and octopole radio frequency voltage 750 V. For negative mode, the MS-TOF parameters included the following: fragmentor 250 V and octopole radio frequency voltage 750 V. During the analyses, two reference masses were used: 121.0509 (purine, detected *m/z* $[C_5H_4N_4+H]^+$) and 922.0098 (HP, detected *m/z* $[C_{18}H_{18}O_6N_3P_3F_{24}+H]^+$) in positive mode and 112.9855 (TFA(NH_4), detected *m/z* $[C_2O_2F_3(NH_4)-H]^-$) and 966.0007 (HP+FA, detected *m/z* $[C_{18}H_{18}O_6N_3P_3F_{24}+FA-H]^-$) in negative mode. The references were continuously infused into the system, enabling constant mass correction. Samples were analyzed in randomized runs, during which they were incubated in an autosampler at 4°C. The analytical runs for both polarities were set up starting with the analysis of ten QCs followed by the samples; a QC sample was injected between blocks of ten samples until the end of the run.

Quality assurance

After data reprocessing, the metabolic features were subsequently filtered. For GC-MS, 82 metabolites were detected. After filtering for a relative standard deviation (RSD) <40 and presence in at least 60% of the samples in each experimental group, 68 metabolites were selected for statistical analysis. For LC-MS, a normalization over the analysis time (injection order) was carried [2]. The detected features were 347 and 335 for ESI+ and ESI-, respectively. Out of them, 261 and 210 features

fulfilled a value of RSD <40, of which 13 and 2 features had not presence in more than 60% of samples in each group, and were discarded. Finally, 248 and 208 features were statistically analyzed for ESI+ and ESI-, respectively.

Metabolite identification

The significant metabolites were identified. In GC-MS the identification was done based on FiehnLib [1] and NIST 14 libraries. In LC-MS the list of accurate masses was searched using the CEU Mass Mediator search tool (http://ceumass.eps.uspceu.es/; error ± 5 ppm) to obtain tentative identifications. Each of them was manually curated based on their MS adducts [3]. In the cases that it was applicable, the elution order was also considered to discard spurious identifications. Eventually the biological role of each compound was evaluated and unrelated identifications such as pesticides, drugs or not possible chemicals structures were excluded. The metabolites are reported in agreement with the criteria of the Metabolomics Standards Initiative [4, 5] with a confidence level grade 2 (putatively annotated compounds), which certitude is increased after manual curation of the final list.

Additional File 2: Principal component analysis (PCA) plot showing clustering of study samples and quality controls. **Abbreviations:** GC-MS, gas chromatography–mass spectrometry; LC-MS, and liquid chromatography–mass spectrometry; ESI, electrospray ionization; PC, principal component.

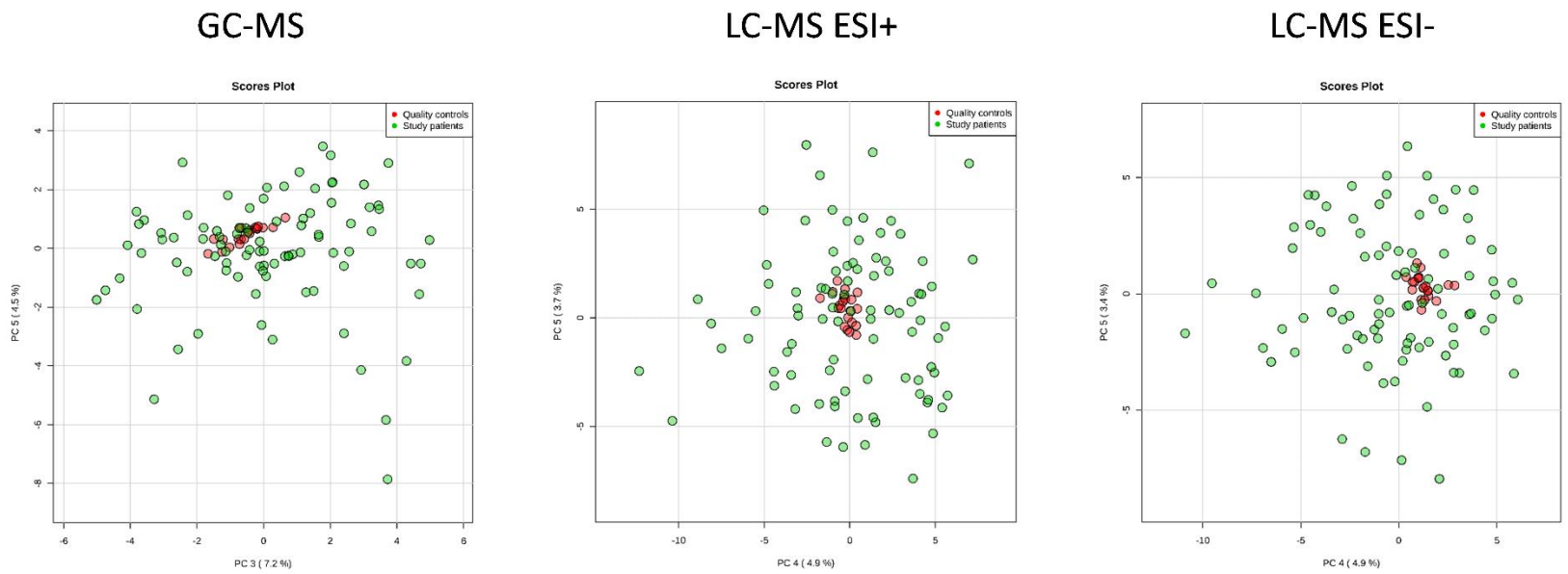

Additional File 3. Multivariate analysis of plasma metabolites regarding HIV coinfection. PLS-DA plot resulting from GC-MS data and metabolites with the highest VIP score (≥1).

Statistics: Multivariate analysis was performed by partial least squares discriminant analysis (PLS-DA). The VIP score measures the variable's importance and allows metabolites to be ranked according to their importance.

Abbreviations: PLS-DA, partial least squares discriminant analysis, VIP, variable importance in projection, GC-MS, gas chromatography–mass spectrometry.

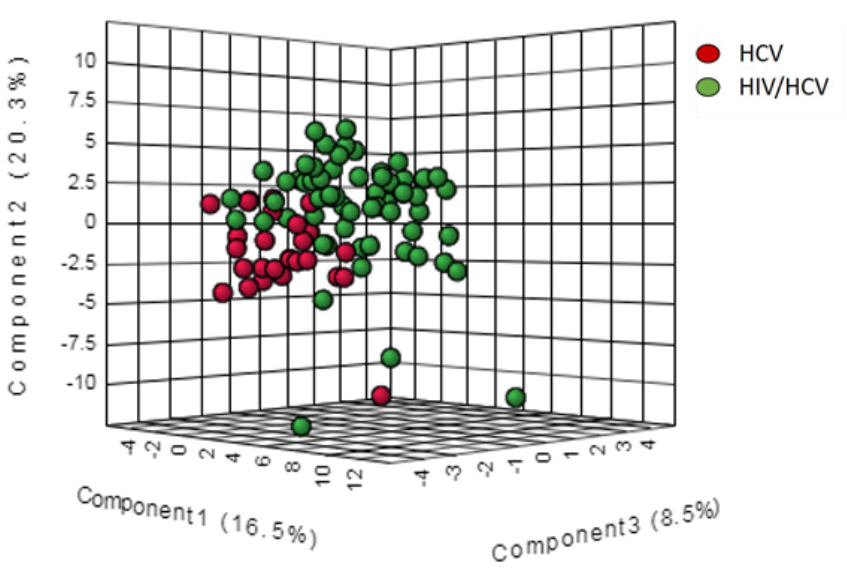

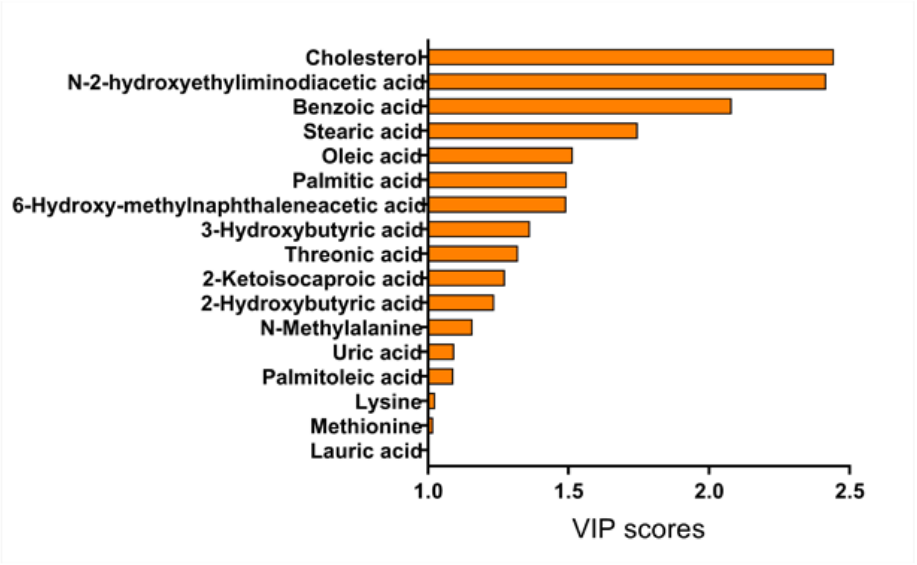

Additional File 4. Summary of associations between metabolites and HIV coinfection (HCV/HIV coinfected vs. HCV monoinfected patients).

		Unadjusted model			Adjusted model		
Metabolite	**Technology**	**OR (95%CI)**	**p-value**	**q-value**	**aOR (95%CI)**	**p-value**	**q-value**
Benzoic acid	GC-MS	0.30 (0.15-0.58)	$3.22*10^{-4}$	**0.007**	0.38 (0.14-1,00)	0.051	0.073
Cholesterol	GC-MS	0.14 (0.05-0.37)	$7.79\text{-}10^{-5}$	**$2.65*10^{-3}$**	0.06 (0.01-0.34)	0.010	**0.023**
N-2-hydroxyethyl-Iminodiacetic acid	GC-MS	2.92 (1.73-4.94)	$6.57*10^{-5}$	**$2.65*10^{-3}$**	2.05 (1.06-3.98)	0.151	0.171
Stearic acid	GC-MS	0.36 (0.20-0.67)	0.001	**0.022**	0.08 (0.01-0.51)	0.009	**0.023**
LPC(16:0)	LC-MS ESI+	2.35(1.36-4.05)	0.002	**0.064**	2.22 (0.86-5.71)	0.044	0.073
LPC (18:0)	LC-MS ESI+	2.61 (1.50-4.56)	$7.62*10^{-4}$	**0.032**	2.78 (1.10-6.99)	0.010	**0.023**
LPC(20:4)	LC-MS ESI+	2.39 (1.34-4.28)	0.003	**0.073**	2.09 (0.80-5.48)	0.316	0.316
PC (16:0/9:0(CHO))	LC-MS ESI+	0.19 (0.09-0.41)	$2.89*10^{-5}$	**$7.17*10^{-3}$**	0.15 (0.05-0.48)	0.008	**0.023**
Acetylcarnitine	LC-MS ESI+	0.35 (0.19-0.63)	$5.62*10^{-5}$	**0.032**	0.22(0.07-0.65)	0.011	**0.023**

Statistics: Values are expressed as odds ratio and 95% confidence interval. P-values were calculated by GLM with binomial distribution (logit-link); q-values represent p-values corrected for multiple testing using the false discovery rate (FDR). Adjusted models were adjusted by the most significant clinical and epidemiological characteristics (see Statistical analysis section). Statistically significant differences are shown in bold.
Abbreviations: OR, odds ratio; aOR, adjusted odds ratio; 95%CI, 95% of confidence interval; p-value, level of significance; q-value, corrected level of significance; PC, phosphatidylcholine; LPC, lysophosphatidylcholine.

Additional File 5. Multivariate analysis of plasma metabolites regarding high alcohol intake (>50 g/day). PLS-DA plot resulting from GC-MS data and metabolites with the highest VIP score (≥1).

Statistics: Multivariate analysis was performed by PLS-DA. The VIP score measures the variable's importance and allows metabolites to be ranked according to their importance.

Abbreviations: PLS-DA, partial least squares discriminant analysis, VIP, variable importance in projection, GC-MS, gas chromatography–mass spectrometry.

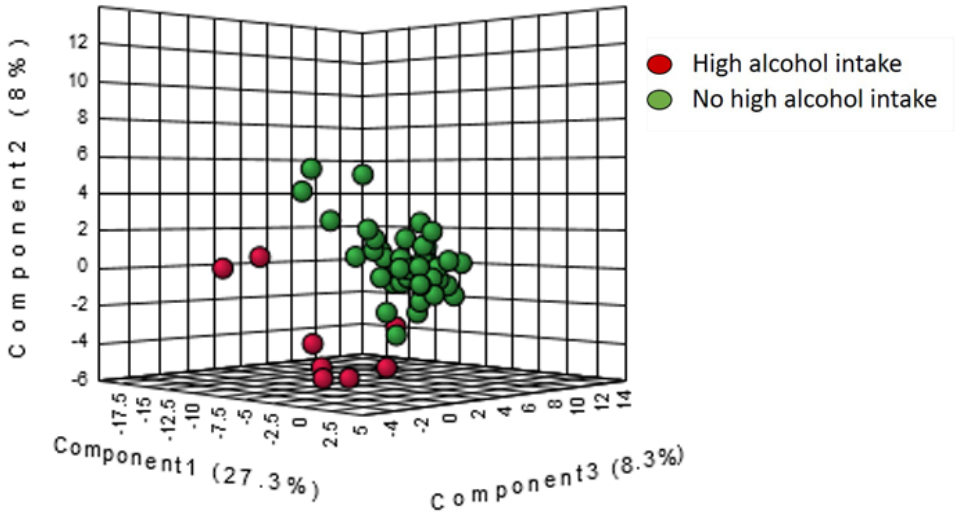

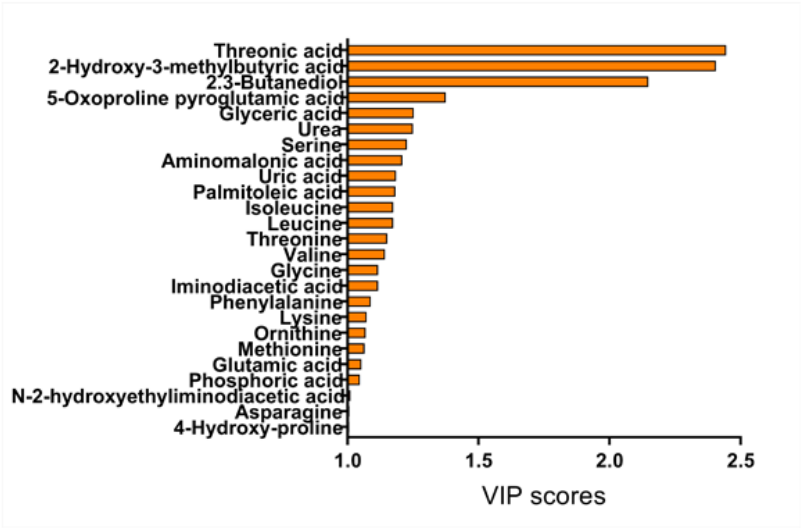

Additional File 6. Summary of associations between plasma metabolites and high alcohol intake (>50 g/day).

		Unadjusted model			Adjusted model		
Metabolite	**Technology**	**OR (95%CI)**	**p-value**	**q-value**	**aOR (95%CI)**	**p-value**	**q-value**
2,3-Butanediol	GC-MS	6.68 (2.04-21.93)	0.002	0.058	60.73 (0.58-6401.83)	0.084	0.084
2-Hydroxy-3-methylbutyric acid	GC-MS	16.63 (2.48-111.42)	0.004	0.085	15.50 (1.96-122.79)	0.009	**0.028**
Threonic.acid	GC-MS	0.17 (0.06-0.49)	0.001	0.058	0.11 (0.01-0.82)	0.064	0.084

Statistics: Values are expressed as odds ratio and 95% confidence interval. P-values were calculated by GLM with binomial distribution (logit-link); q-values represent p-values corrected for multiple testing using the false discovery rate (FDR). Adjusted models were adjusted by the most significant clinical and epidemiological characteristics (see Statistical analysis section). Statistically significant differences are shown in bold.
Abbreviations: OR, odds ratio; aOR, adjusted odds ratio; 95%CI, 95% of confidence interval; p-value, level of significance; q-value, corrected level of significance.

Additional File 7. Summary of associations between metabolites and previous HCV therapy failure.

				Unadjusted model					Adjusted model					
Feature	**Technology**	**Mass**	**RT (min)**	**OR**	**IC2.5**	**IC97.5**	**p**	**q**	**aOR**	**IC2.5**	**IC97.5**	**p**	**q**	**Identification**
210.1607.0.25500023	LC-MS-	210.1607	0.25500023	0.39	0.22	0.67	6.6×10^{-4}	0.072	0.39	0.22	0.68	8.6×10^{-4}	0.074	Unknown
191.1076.0.25500023	LC-MS-	191.1076	0.25500023	0.39	0.23	0.67	6.9×10^{-4}	0.072	0.37	0.21	0.66	7.5×10^{-4}	0.074	Unknown

Statistics: Values are expressed as odds *ratio* and 95% confidence interval. P-values were calculated by GLM model with binomial distribution; q-values represent p-values corrected for multiple testing using the false discovery rate (FDR). Adjusted models were adjusted by the most significant clinical and epidemiological characteristics (see Statistical analysis section). Statistically significant differences are shown in bold. **Abbreviations**: OR, odds ratio; aOR, adjusted odds ratio; 95%CI, 95% of confidence interval; p-value, level of significance; q-value, corrected level of significance.

Additional File 8. Permutation by separation distance (B/W) to confirm the validity of the PLS-DA models, with a permutation number of 1000. **Abbreviations:** GC-MS, gas chromatography–mass spectrometry; LC-MS, and liquid chromatography–mass spectrometry; ESI, electrospray ionization.

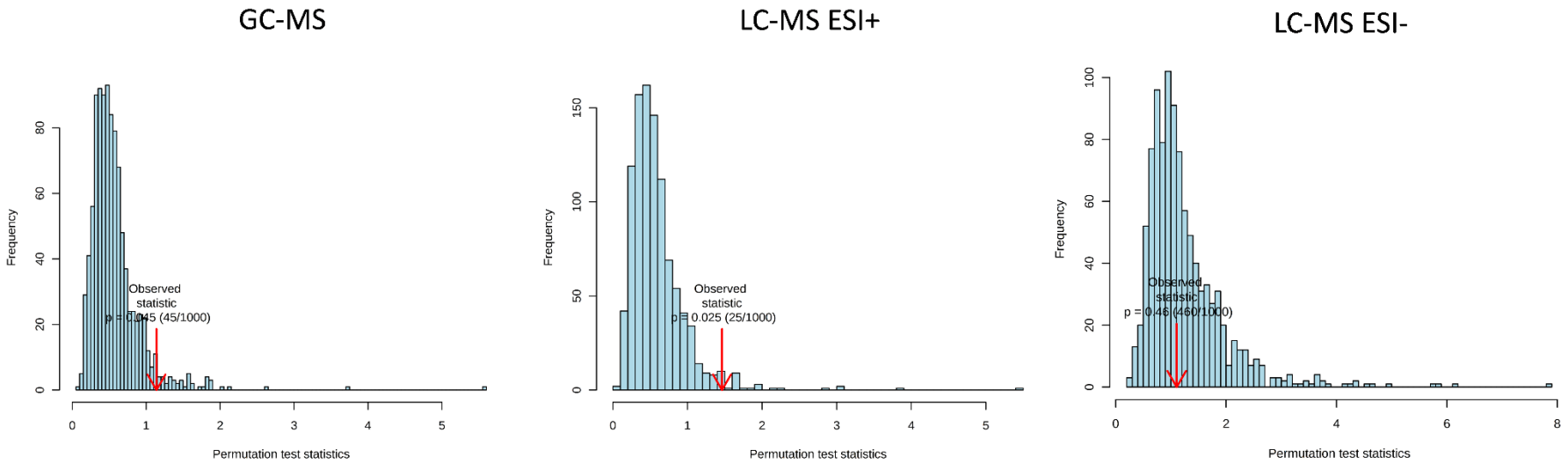

Additional File 9. Summary of the highest variable importance in projection (VIP) scores for the multivariate analysis of metabolites according to the CTP score. **Statistics:** Partial least squares discriminant analysis (PLS-DA) was used to calculate the VIP score for each of the metabolites. The VIP score measures the variable's importance and allows ranking of the metabolites according to their importance. **Abbreviations:** GC-MS, gas chromatography–mass spectrometry; LC-MS, and liquid chromatography–mass spectrometry; ESI, electrospray ionization; PC, phosphatidylcholine; LPC, lysophosphatidylcholine; LPE, lysophosphatidylethanolamine.

GC-MS

Metabolites	**VIP score**
Glycolic acid	2.2855
2-Ketoisocaproic acid	1.6336
2-Hydroxy-3-methylbutyric acid	1.5122
Palmitoleic acid	1.4778
Oleic acid	1.4708
Methionine	1.4646
Palmitic acid	1.4551
2.3-Butanediol	1.4459
2-Hydroxybutyric acid	1.3753
Tyrosine	1.3550
Threonic acid	1.2964
Stearic acid	1.2279
Glycerol	1.1796
3-Hydroxybutyric acid	1.1705
N-2-hydroxyethyliminodiacetic acid	1.1661
Aminomalonic acid	1.1417
Lauric acid	1.1333
Succinic acid	1.1205
p-Cresol	1.0294
5-Oxoproline (pyroglutamic acid)	1.0063

LC-MS ESI+

Metabolites	**VIP score**
Carnitine	2.3015
LPC(16:0)	2.2998
LPC(20:4)	1.9704
LPC(18:0)	1.9362
LPE(22:6)	1.8365
LPC(20:3)	1.7856
LPC(22:6)	1.6811
PC(16:0/9:0(CHO))	1.6452
Acetylcarnitine	1.6136
2-amino-3-methylbutanol/Neurine	1.1557
LPC(16:1)	1.0196

Additional File 10. Association between individual metabolites and CTP score. **Statistics:** Ordinal regression models (dependent variable: CTP score; independent variable: metabolites), adjusted by the most relevant covariates (see Statistical analysis in Patients and methods section). *P*-values were adjusted by FDR correction for multiple comparisons (Benjamini and Hochberg). **Abbreviation**s: RT, retention time; OR, odd ratio; CI, confidence interval; p-value, level of significance; q-value, adjusted p-value by FDR correction; LPC, lysophosphatidylcholine.

				Unadjusted model					Adjusted model					
Feature	**Technology**	**Mass**	**RT (min)**	**OR**	**IC2.5**	**IC97.5**	**p**	**q**	**aOR**	**IC2.5**	**IC97.5**	**p**	**q**	**Identification**
X2.3.Butanediol	GC-MS	NA	NA	1.65	1.06	2.59	0.027	0.326						
X2.Hydroxy.3.methylbutyric.acid	GC-MS	NA	NA	1.72	1.12	2.68	0.014	0.323						
X2.Hydroxybutyric.acid	GC-MS	NA	NA	1.60	1.03	2.57	0.040	0.326						
X2.Ketoisocaproic.acid	GC-MS	NA	NA	0.63	0.40	0.96	0.037	0.326						
Glycolic.acid	GC-MS	NA	NA	2.35	1.44	3.98	0.001	**0.058**	2.66	1.56	4.87	0.000	**0.001**	Glycolic acid
Oleic.acid	GC-MS	NA	NA	1.71	1.06	2.89	0.036	0.326						
Palmitoleic.acid	GC-MS	NA	NA	2.02	1.19	3.68	0.014	0.323						
Threonic.acid	GC-MS	NA	NA	1.79	1.07	3.25	0.037	0.326						
Unknown_11.04	GC-MS	NA	NA	0.65	0.43	0.99	0.043	0.326						
X495.3332.5.817994	LC-MS ESI+	495.3332	5.817994	0.38	0.21	0.64	0.001	**0.027**	0.32	0.16	0.59	0.000	**0.001**	LPC(16:0) d
X545.3479.5.8089995	LC-MS ESI+	545.3479	5.8089995	0.45	0.25	0.75	0.004	**0.082**	0.36	0.18	0.65	0.001	**0.0023**	LysoPC(20:3)
X103.0998.5.8220115	LC-MS ESI+	103.0998	5.8220115	0.41	0.24	0.65	0.000	**0.027**	0.34	0.19	0.59	0.000	**0.001**	Unknown
X543.3325.5.4619956	LC-MS ESI+	543.3325	5.4619956	0.41	0.22	0.70	0.002	**0.064**	0.49	0.25	0.91	0.032	0.035	LysoPC(20:4) d
X523.3638.6.3559937	LC-MS ESI+	523.3638	6.3559937	0.47	0.28	0.76	0.003	**0.072**	0.42	0.24	0.70	0.001	**0.002**	PC(18:0/0:0)

X495.3325.5.666006	LC-MS ESI+	495.3325	5.666006	0.37	0.21	0.63	0.000	**0.027**	0.32	0.16	0.59	0.000	**0.001**	PC(16:0/0:0)
X543.3322.5.5649934	LC-MS ESI+	543.3322	5.5649934	0.39	0.21	0.67	0.001	**0.044**	0.39	0.21	0.69	0.002	**0.003**	LysoPC(20:4)
X444.3049.0.28200057	LC-MS ESI+	444.3049	0.28200057	0.53	0.29	0.90	0.027	0.413						
X523.3639.6.5389843	LC-MS ESI+	523.3639	6.5389843	0.48	0.28	0.78	0.004	**0.082**	0.43	0.24	0.71	0.0017	**0.0023**	PC(18:0/0:0) d
X567.3322.5.5489993	LC-MS ESI+	567.3322	5.5489993	0.44	0.25	0.73	0.002	**0.064**	0.32	0.17	0.57	0.000	**0.001**	PC(22:6/0:0)
X1080.6339.5.817994	LC-MS ESI+	1080.633	5.817994	0.40	0.23	0.65	0.000	**0.027**	0.33	0.17	0.58	0.000	**0.001**	Unknown
X585.3021.5.818982	LC-MS ESI+	585.3021	5.818982	0.40	0.23	0.65	0.000	**0.027**	0.33	0.17	0.59	0.000	**0.001**	Unknown
X161.1048.0.31000045	LC-MS ESI+	161.1048	0.31000045	1.80	1.13	2.90	0.013	0.221						
X203.1169.0.30899903	LC-MS ESI+	203.1169	0.30899903	1.62	1.03	2.63	0.043	0.445						
X532.3545.0.2809992	LC-MS ESI+	532.3545	0.2809992	0.61	0.37	0.98	0.049	0.486						
X488.3314.0.28200057	LC-MS ESI+	488.3314	0.28200057	0.57	0.33	0.94	0.035	0.445						
X183.0871.0.29700062	LC-MS ESI+	183.0871	0.29700062	1.65	1.03	2.67	0.037	0.445						
X117.0789.0.3079994	LC-MS ESI+	117.0789	0.3079994	1.65	1.02	2.70	0.043	0.445						
X103.0999.6.541007	LC-MS ESI+	103.0999	6.541007	0.50	0.30	0.80	0.005	**0.097**	0.59	0.33	1.04	0.069	0.069	Unknown
X649.4327.6.779012	LC-MS ESI+	649.4327	6.779012	1.72	1.05	2.96	0.040	0.445						
X185.204.0.26200023	LC-MS ESI+	185.204	0.26200023	0.63	0.40	0.98	0.042	0.445						
X664.4305.0.2809992	LC-MS ESI+	664.4305	0.2809992	0.58	0.34	0.93	0.029	0.428						
X121.9565.0.34299982	LC-MS ESI+	121.9565	0.34299982	0.59	0.35	0.94	0.033	0.445						
X103.0997.6.3559937	LC-MS ESI+	103.0997	6.3559937	0.42	0.25	0.69	0.001	**0.031**	0.38	0.21	0.63	0.000	**0.001**	Unknown
X525.2854.5.403004	LC-MS ESI+	525.2854	5.403004	0.48	0.29	0.76	0.003	**0.067**	0.46	0.26	0.78	0.005	0.006	PE(22:6/0:0)
X130.063.0.25799963	LC-MS ESI-	130.063	0.25799963	0.61	0.34	0.88	0.020	0.480						
X472.062.0.26200023	LC-MS ESI-	472.062	0.26200023	0.59	0.36	0.91	0.022	0.480						
X546.0626.0.2589997	LC-MS ESI-	546.0626	0.2589997	0.63	0.39	0.99	0.048	0.577						
X196.1455.0.257	LC-MS ESI-	196.1455	0.257	0.60	0.35	0.97	0.047	0.577						
X194.1293.0.25500023	LC-MS ESI-	194.1293	0.25500023	0.56	0.33	0.90	0.021	0.480						
X515.2919.3.5839999	LC-MS ESI-	515.2919	3.5839999	2.63	1.58	4.65	0.000	**0.084**	3.62	1.96	7.30	0.000	**0.001**	Taurocholic acid

X113.9929.0.22700024	LC-MS ESI-	113.9929	0.22700024	0.60	0.38	0.93	0.023	0.480						
X482.0907.0.2560003	LC-MS ESI-	482.0907	0.2560003	0.60	0.38	0.93	0.024	0.480						
X184.1087.0.257	LC-MS ESI-	184.1087	087.0.257	0.59	0.37	0.93	0.026	0.480						
X108.0572.0.24200036	LC-MS ESI-	108.0572	0.24200036	0.60	0.37	0.94	0.028	0.480						
X220.8528.0.41899928	LC-MS ESI-	220.8528	0.41899928	1.65	1.03	2.77	0.045	0.577						
X183.9957.0.22900008	LC-MS ESI-	183.9957	0.22900008	0.55	0.35	0.87	0.011	0.480						
X574.0573.2.8510072	LC-MS ESI-	574.0573	2.8510072	1.81	1.11	2.98	0.018	0.480						
X173.9992.0.24000041	LC-MS ESI-	173.9992	0.24000041	0.54	0.35	0.82	0.004	0.412						
X150.0167.9.493017	LC-MS ESI-	150.0167	9.493017	0.56	0.32	0.90	0.020	0.480						
X240.0702.9.838995	LC-MS ESI-	240.0702	9.838995	0.61	0.38	0.96	0.037	0.546						
X427.9751.0.27199957	LC-MS ESI-	427.9751	0.27199957	0.60	0.37	0.95	0.033	0.531						

Additional File 11. Summary of unadjusted and adjusted associations between plasma metabolites and hepatic decompensation (CTP ≥7).

		Unadjusted model			Adjusted model		
Metabolite	**Technology**	**OR (95%CI)**	**p-value**	**q-value**	**aOR (95%CI)**	**p-value**	**q-value**
Glycolic acid	GC-MS	3,09 (1.55-6.16)	0.001	**0.011**	6.28 (1.74; 22.62)	0.005	**0,020**
LPC(20:3)	LC-MS ESI+	0.64 (0,34-1,20)	0.165	0.220	0.06 (0.01-0.62)	0.018	**0.032**
LPC(18:0)	LC-MS ESI+	0.54 (0.29-1.02)	0.058	0.116	0.40 (0.13-1.25)	0.114	0.151
LPC(16:0)	LC-MS ESI+	0.45 (0.23-0.89)	0,021	0.055	0.11 (0.02-0.51)	0.005	**0.020**
LPC(20:4)	LC-MS ESI+	0.61 (0.32-1.17)	0.137	0.219	0.03 (0.01-0.59)	0.020	**0.032**
LPC(22:6)	LC-MS ESI+	0.79 (0.43-1.44)	0.441	0.441	0.65 (0.28-1.47)	0.295	0.295
LPE (22:6)	LC-MS ESI+	0.70 (0.40-1.26)	0.235	0.269	0.67 (0.32-1.41)	0.287	0.295
Taurocholic acid	LC-MS ESI-	2.91 (1.42-5.97)	0.004	**0.014**	4.52 (1.47-13.90)	0.009	**0.023**

Statistics: Values are expressed as odds ratio and 95% confidence interval. P-values were calculated by GLM model with binomial distribution; q-values represent p-values corrected for multiple testing using the false discovery rate (FDR). Adjusted models were adjusted by the most significant clinical and epidemiological characteristics (see Statistical analysis section). Statistically significant differences are shown in bold. **Abbreviations**: OR, odds ratio; aOR, adjusted odds ratio; 95%CI, 95% of confidence interval; p-value, level of significance; q-value, corrected level of significance; LPC, lysophosphatidylcholine; LPE, lysophosphatidylethanolamine.

Additional File 12. Correlation between bacteria-related metabolites and bacterial translocation and infection.

	LPS		LBP		IL6	
Metabolite	**r**	***p***	**r**	***p***	**r**	***p***
2-Hydroxybutyric acid	-0.017	0.871	0.118	0.269	-0.008	0.937
3-Hydroxybutyric acid	-0.060	0.572	0.265	**0.012**	0.175	0.099
2-Hydroxy-3-methylbutyric acid	-0.091	0.392	0.065	0.540	0.278	**0.008**
2,3-Butanediol	-0.063	0.558	-0.011	0.918	0.362	**<0.001**
N-(2-hydroxyethyl) iminodiacetic acid	0.254	**0.016**	0.012	0.914	-0.011	0.921

Statistics: *P*-values were calculated by Sparman correlation. Statistically significant differences are shown in bold. **Abbreviations**: r, Spearman correlation coefficient; p, level of significance; LPS, lipopolysaccharide; LBP, lipopolysaccharide binding protein; IL6, interleukin 6.